

Hydrogeology and Hydrochemistry of the Midnite Mine, Northeastern Washington

By A. D. Marcy, B. J. Scheibner, K. L. Toews,
and C. M. K. Boldt

UNITED STATES DEPARTMENT OF THE INTERIOR



BUREAU OF MINES

*U.S. Department of the Interior
Mission Statement*

As the Nation's principal conservation agency, the Department of the Interior has responsibility for most of our nationally-owned public lands and natural resources. This includes fostering sound use of our land and water resources; protecting our fish, wildlife, and biological diversity; preserving the environmental and cultural values of our national parks and historical places; and providing for the enjoyment of life through outdoor recreation. The Department assesses our energy and mineral resources and works to ensure that their development is in the best interests of all our people by encouraging stewardship and citizen participation in their care. The Department also has a major responsibility for American Indian reservation communities and for people who live in island territories under U.S. administration.

Report of Investigations 9484

**Hydrogeology and Hydrochemistry
of the Midnite Mine, Northeastern
Washington**

**By A. D. Marcy, B. J. Scheibner, K. L. Toews,
and C. M. K. Boldt**

**UNITED STATES DEPARTMENT OF THE INTERIOR
Bruce Babbitt, Secretary**

BUREAU OF MINES

Library of Congress Cataloging in Publication Data:

Hydrogeology and hydrochemistry of the Midnite Mine, Northeastern Washington
/ by A.D. Marcy ... [et al.].

p. cm. — (Report of investigations; 9484)

Includes bibliographical references (p. 28).

1. Water quality—Washington (State)—Spokane Indian Reservation. 2. Ground-water flow—Washington (State)—Spokane Indian Reservation. 3. Acid mine drainage—Environmental aspects—Washington (State)—Spokane Indian Reservation. 4. Uranium mines and mining—Environmental aspects—Washington (State)—Spokane Indian Reservation. I. Marcy, A. D. (Allen Dale). II. Title: Midnite Mine, Wellpinit, WA. III. Series: Report of investigations (United States. Bureau of Mines); 9484.

TN23.U43 [TD224.W2] 622 s—dc20 [628.1'6832'0979723] 93-3159
CIP

CONTENTS

	<i>Page</i>
Abstract	1
Introduction	2
Background	2
Site description	2
Site geology	6
Acknowledgments	7
Methods	7
Field	7
Laboratory	9
Data collection	10
Ground water elevations and flow paths	10
Computer modeling methods	10
Presentation and interpretation of data	12
Rainwater	15
Well 89-6	15
Comparison of rainwater and water from well 89-6	15
Well 89-5D	15
Blood Pool	16
Boyd Seep	17
Temporal variations in water quality	17
Possible flow path	18
Drainage from protore pile	20
Pit 3	21
Pit 3 seep	21
Well 89-3	22
Well 89-4	23
Temporal changes	23
Proposed flow path from well 89-4S to South Spoils Seep	24
East Drainage surface runoff	25
West Drainage	26
Conclusions	26
Recommendations for future research	27
References	28
Appendix.—Data used in ground water modeling	29

ILLUSTRATIONS

1. Aerial view showing sampling locations	3
2. Aerial view showing extent of mining in 1976	4
3. Aerial view showing extent of mining in 1980	5
4. North-south cross section across Midnite Mine	6
5. Details of well completion at seven sampling locations	8
6. Ground water elevation contours	11
7. Temporal variations in ground water quality at Boyd Seep	17
8. Temporal variations in mass of released metals at Boyd Seep	18
9. Temporal variations in water level and pH	22
10. Temporal variations in ground water quality at well 89-3M	23
11. Temporal variations in ground water quality at well 89-3D	23
12. Temporal variations in water level and ground water quality at well 89-4S	24
13. Temporal variations in calcium, magnesium, and sulfate	25

TABLES

	<i>Page</i>
1. Instrument calibration accuracy	9
2. Possible minerals and gases used as input for BALANCE program	12
3. Water quality data	13
A-1. Saturation indices for selected minerals from WATEQ4F using analytical data from well 89-6 and well 89-5D	29
A-2. Input and output files from BALANCE comparing rainwater and water from well 89-6	29
A-3. Mineral and gas input data to BALANCE comparing rainwater and water from well 89-6	29
A-4. Mineral and gas output data from BALANCE comparing rainwater and water from well 89-6	29
A-5. Input and output files from BALANCE evaluating possible flow path from well 89-6 to well 89-5D	30
A-6. Mineral and gas input data to BALANCE evaluating possible flow path from well 89-6 to well 89-5D	30
A-7. Mineral and gas output data from BALANCE evaluating possible flow path from well 89-6 to well 89-5D	30
A-8. Saturation indices for selected minerals from WATEQ4F using analytical data from Blood Pool	30
A-9. Input and output files from BALANCE evaluating change of well 89-6-type water into Blood Pool water	31
A-10. Mineral and gas input data to BALANCE evaluating change of well 89-6-type water into Blood Pool water	31
A-11. Mineral and gas output data from BALANCE evaluating change of well 89-6-type water into Blood Pool water	31
A-12. Saturation indices for selected minerals from WATEQ4F using analytical data from pit 3, Boyd Seep, well 89-1S, and well 89-1M	31
A-13. Input and output files from BALANCE evaluating flow path from pit 3 to Boyd Seep	32
A-14. Mineral and gas input data to BALANCE evaluating flow path from pit 3 to Boyd Seep	32
A-15. Mineral and gas output data from BALANCE evaluating flow path from pit 3 to Boyd Seep	32
A-16. Input and output files from BALANCE evaluating flow path from well 89-1S to Boyd Seep with mixing of water from well 89-1M	32
A-17. Mineral and gas input data to BALANCE evaluating flow path from well 89-1S to Boyd Seep with mixing of water from well 89-1M	33
A-18. Mineral and gas output data for model 8A from BALANCE evaluating flow path from well 89-1S to Boyd Seep with mixing of water from well 89-1M	33
A-19. Input and output files from BALANCE evaluating mixing of water from well 89-1S with well 89-6-type water to obtain water similar to that found at Boyd Seep	33
A-20. Mineral and gas input data to BALANCE evaluating mixing of water from well 89-1S with well 89-6-type water to obtain water similar to that found at Boyd Seep	33
A-21. Mineral and gas output data from BALANCE evaluating mixing of water from well 89-1S with well 89-6-type water to obtain water similar to that found at Boyd Seep	34
A-22. Input and output files from BALANCE evaluating mixing of water from well 89-1S with well 89-6-type water to obtain water similar to that found at Boyd Seep using alternative mineral data	34
A-23. Mineral and gas input data to BALANCE evaluating mixing of water from well 89-1S with well 89-6-type water to obtain water similar to that found at Boyd Seep using alternative mineral data	34
A-24. Mineral and gas output data for model 10A from BALANCE evaluating mixing of water from well 89-1S with well 89-6-type water to obtain water similar to that found at Boyd Seep using alternative mineral data	35
A-25. Saturation indices for selected minerals from WATEQ4F using analytical data from Sis Pool	35
A-26. Input and output files from BALANCE evaluating quantity of minerals consumed in protore pile to produce water at Sis Pool from infiltration water	35
A-27. Mineral and gas input data to BALANCE evaluating quantity of minerals consumed in protore pile to produce water at Sis Pool from infiltration water	35
A-28. Mineral and gas output data for model 12A from BALANCE evaluating quantity of minerals consumed in protore pile to produce water at Sis Pool from infiltration water	35
A-29. Input and output files from BALANCE comparing mixing ratios of infiltration water and pumpback water from pollution control pond to produce water found in pit 3	36

TABLES—Continued

	<i>Page</i>
A-30. Mineral and gas input data to BALANCE comparing mixing ratios of infiltration water and pumpback water from pollution control pond to produce water found in pit 3	36
A-31. Mineral and gas output data for model 13A from BALANCE comparing mixing ratios of infiltration water and pumpback water from pollution control pond to produce water found in pit 3	36
A-32. Saturation indices for selected minerals from WATEQ4F using analytical data from pit 4 and pit 3 seep ..	36
A-33. Input and output files from BALANCE evaluating possible flow path from pit 4 to pit 3 seep with mixing of well 89-6 water	37
A-34. Mineral and gas input data to BALANCE evaluating possible flow path from pit 4 to pit 3 seep with mixing of well 89-6 water	37
A-35. Mineral and gas output data from BALANCE evaluating possible flow path from pit 4 to pit 3 seep with mixing of well 89-6 water	37
A-36. Saturation indices for selected minerals from WATEQ4F using analytical data from well 89-3M and well 89-3D	38
A-37. Saturation indices for selected minerals from WATEQ4F using analytical data from well 89-4S and South Spoils Seep	38
A-38. Input and output files from BALANCE evaluating possible flow path from well 89-4S to South Spoils Seep with mixing of well 89-6-type water	38
A-39. Mineral and gas input data to BALANCE evaluating possible flow path from well 89-4S to South Spoils Seep with mixing of well 89-6-type water	38
A-40. Mineral and gas output data for model 18A from BALANCE evaluating possible flow path from well 89-4S to South Spoils Seep with mixing of well 89-6-type water	38
A-41. Saturation indices for selected minerals from WATEQ4F using analytical data from East Drainage Control and East Drainage 11	39
A-42. Input and output files from BALANCE evaluating flow path from East Drainage Control to East Drainage 11 with mixing of water from Boyd Seep	39
A-43. Mineral and gas input data to BALANCE evaluating flow path from East Drainage Control to East Drainage 11 with mixing of water from Boyd Seep	39
A-44. Mineral and gas output data for model 20A from BALANCE evaluating flow path from East Drainage Control to East Drainage 11 with mixing of water from Boyd Seep	40
A-45. Saturation indices for selected minerals from WATEQ4F using analytical data from West Drainage Control and well 89-7	40

UNIT OF MEASURE ABBREVIATIONS USED IN THIS REPORT

cm	centimeter	m	meter
ft	foot	mg/L	milligram per liter
gal	gallon	min	minute
gal/min	gallon per minute	mL	milliliter
gal/yr	gallon per year	mL/min	milliliter per minute
g/d	gram per day	mM	millimolar
ha	hectare	mm	millimeter
in	inch	μ m	micrometer
kg	kilogram	mol	mole
km	kilometer	mS/m	millisiemens per meter
L	liter	mV	millivolt
L/min	liter per minute	pct	percent
L/yr	liter per year	yd	yard

HYDROGEOLOGY AND HYDROCHEMISTRY OF THE MIDNITE MINE, NORTHEASTERN WASHINGTON

By A. D. Marcy,¹ B. J. Scheibner,² K. L. Toews,³ and C. M. K. Boldt⁴

ABSTRACT

The Midnite Mine is an inactive, hard-rock uranium mine in Stevens County, WA. Oxidation of sulfide-containing minerals, primarily pyrite, in the ore body produces large quantities of acidic water. An interception system installed by the mining company limits the discharge of contaminated water from the mine. The U.S. Bureau of Indian Affairs (BIA) and the U.S. Bureau of Land Management (BLM) have been actively involved in planning remediation of the disturbed areas. To assist in remediation, the U.S. Bureau of Mines (USBM) initiated research to determine water quality and to define ground water flow characteristics. USBM personnel designed a monitoring network, supervised installation of sampling wells, and collected and analyzed water samples. This Report of Investigations describes interpretation of data collected between December 1989 and April 1992. The computer program WATEQ4F was used to identify aqueous species distribution and to calculate potential solid phase controls of solubility. To assist in interpretation of changes in water quality between sampling locations and to develop models describing proposed flow paths, the computer program BALANCE was used. Using output from these programs and field observations, a description of the chemistry along proposed ground water flow paths at the mine is presented.

¹Chemist.

²Geologist.

³Engineering technician.

⁴Civil engineer.

Spokane Research Center, U.S. Bureau of Mines, Spokane, WA.

INTRODUCTION

The Midnite Mine is an inactive, hard-rock uranium mine located on the Spokane Indian Reservation, Stevens County, WA, approximately 64 km (40 miles) northwest of Spokane and 13 km (8 miles) northwest of Wellpinit. The site was leased by Dawn Mining Co. in 1954 and included 328 ha (811 acres), of which 130 ha (321 acres) (an area about 0.8 km [0.5 mile] wide and 1.6 km [1 mile] long) was developed during mining operations. The mine ceased operations in 1981, leaving two open pits, several waste rock piles, and stockpiles of low-grade uranium ore (protore). An aerial view of the site taken in 1982 is shown in figure 1. Figures 2 and 3 show the extent of mining activities in 1976 and 1980, respectively.

Since mining operations stopped, BIA and BLM have been actively involved in planning remediation of the disturbed areas. Such remediation efforts are necessary because oxidation of pyrite and other sulfide minerals in the ore body forms acids that leach toxic metals, including radium and uranium, through the disturbed area.

As public concern about the quality of the environment has increased, USBM has focused more of its research on methods to minimize the environmental impact of

mining activities. To assist BIA and BLM at the Midnite Mine, in 1988 USBM initiated an investigation of water-rock interactions at the mine. The ground water flow system and the leaching characteristics of wastes have significant effects on the quantity and quality of water at the mine and impact the quality of water leaving the mine. Therefore, a thorough hydrogeological and hydrochemical characterization of the minesite is required to assist in designing appropriate remediation and reclamation activities. Researchers at USBM's Spokane Research Center (SRC) designed a monitoring network, supervised installation of sampling wells, and collected and analyzed samples.

The purpose of the present research is to determine water quality and define ground water flow characteristics at the Midnite Mine as part of the effort in developing a reclamation plan. The knowledge gained from a detailed investigation of the behavior of contaminants at this site will have general applicability to other hard-rock mines. In addition, the design and sampling techniques can be applied to future field work and used in other ongoing research.

BACKGROUND

SITE DESCRIPTION

Altitude of the mine ranges from 1,036 m (3,400 ft) above mean sea level at the northern end to 730 m (2,400 ft) at the southern end (fig. 4). During the period the mine was active, six pits or subpits were opened. Four of these were subsequently backfilled with overburden and waste as mining progressed, while two pits (3 and 4) were left open (fig. 1). The present bottom of pit 3 is about 130 m (430 ft) lower in elevation than the bottom of pit 4 (fig. 4). Pit 3 contains approximately 1,628 million L (430 million gal) of water and is more contaminated than pit 4. Pit 4 contains approximately 265 million L (70 million gal) of water, much of which had been pumped from pit 3 during dewatering operations that began around 1979; as of June 1992, approximately 1,893 million L (500 million gal) of acidic waters have accumulated in the two pits at a rate of 95 to 189 million L/yr (25 to 50 million gal/yr). The water level in pit 4 remains fairly constant, responding only to seasonal variations. The water level in pit 3 is constantly rising because of precipitation and infiltration and because water is being pumped into it from the pollution control pond.

Many waste rock piles and eight low-grade ore (protore) piles remain on the minesite. The two largest waste rock piles are southwest of pit 4 and about 457 m (500 yd)

south of pit 3. These have been designated Hillside Spoils and South Spoils, respectively. The pollution control pond was constructed in 1979 below South Spoils to intercept seepage from the spoils (fig. 4). Water from other seeps that have formed since that time are pumped to the pollution control pond and then to pit 3.

The climate is continental type, with warm, dry summers and cold winters. Precipitation at Wellpinit averaged 473 mm from 1951 through 1980; from spring through fall, it comes as rain, while in winter, it is mostly in the form of snow. Local vegetation consists of grasses, light brush, and coniferous forest, mainly ponderosa pine [Sumioka, 1991 (22)].⁵

Recharge to the site consists of rainfall and snowmelt from the immediate vicinity. Discharge consists of evaporation, surface stream runoff, and a small amount of ground water flow [Sumioka, 1991 (22)]. Two tributaries to Blue Creek carry most of the water from the site; these streams were informally designated East Drainage and West Drainage. Several sampling locations are shown in figures 1 through 4 to provide perspective on present water movement in relation to ancestral drainages. East

⁵Italic numbers in parentheses refer to items in the list of references preceding the appendix at the end of this report.



Figure 1.—Aerial view showing sampling locations. (Circles = well numbers; squares = surface sites.)



Figure 2.—Aerial view showing extent of mining in 1976.

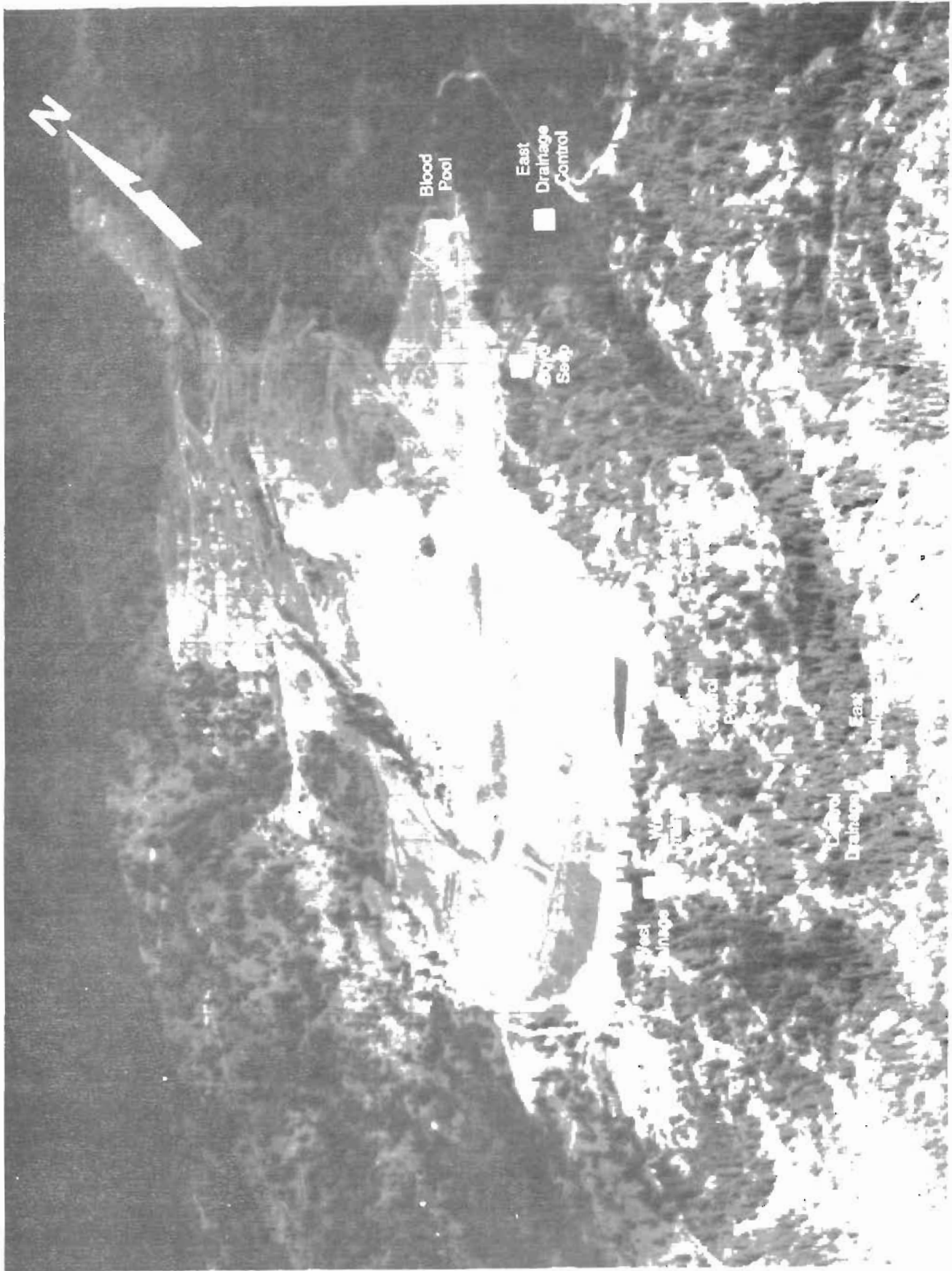


Figure 3.—Aerial view showing extent of mining in 1980.

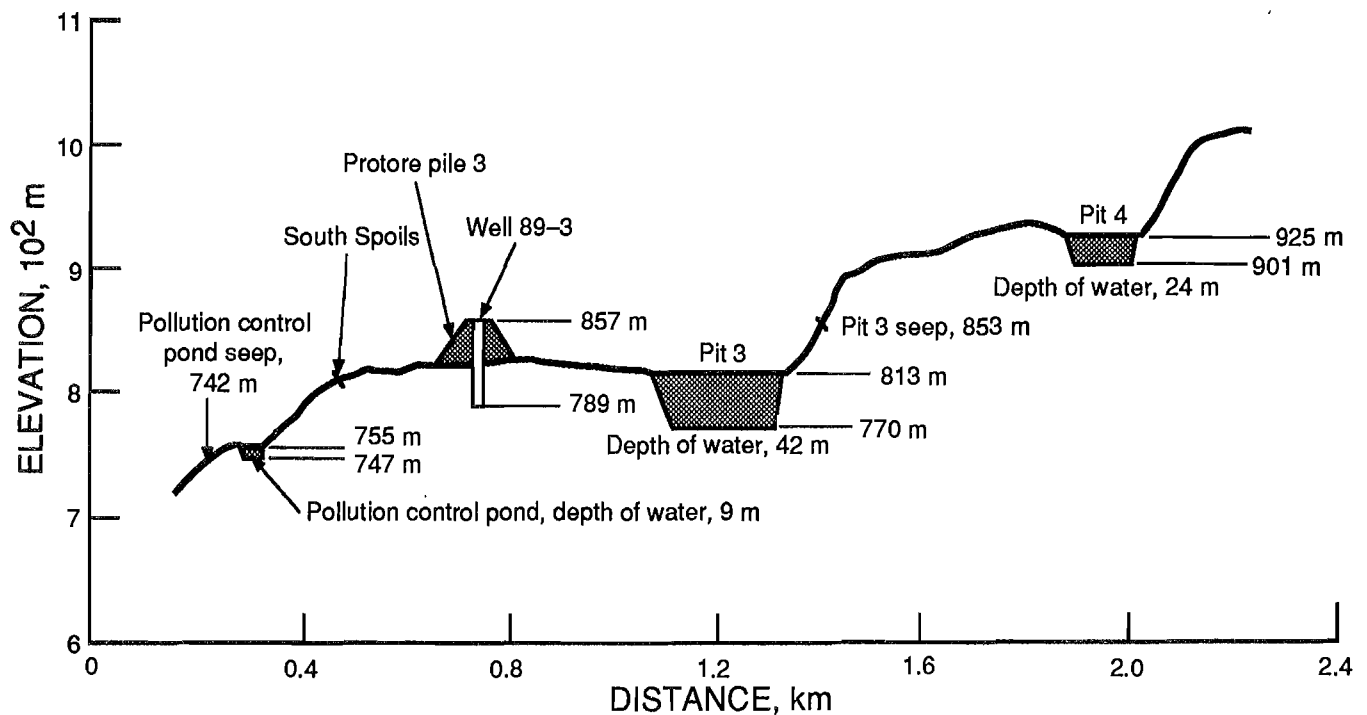


Figure 4.—North-south cross section across Midnite Mine. (Vertical exaggeration, 2.4 times.) (Blood Pool elevation = 829 m; Boyd Seep elevation = 805 m.)

Drainage flows east of pit 4, pit 3, and Blood Pool through the East Drainage Control sampling location and into Blue Creek. West Drainage has been changed because of mining activities, but it flows generally north-south from the base of the pit 4-Hillside Spoils area along the western flank of the ground disturbed by mining. From there, it flows generally southeast to its confluence with East Drainage. The sampling locations are in the western flank of the disturbed area.

SITE GEOLOGY

The Midnite Mine lies on the southwestern slope of Spokane Mountain at the southern end of the Huckleberry Mountains, a minor range in the north-south-trending Selkirk system. It is located on the western edge of a 1.6-km- (1-mile) wide roof pendant of the metasedimentary Togo Formation of the Belt Supergroup. This Precambrian sequence is about 183 m (600 ft) thick in the area and contains graphite-bearing argillite, schist, and phyllite with interbeds of marble, calc-silicate, and quartzite [Ludwig, Nash, and Naeser, 1981 (8)]. The bedding strikes generally N. 10° W. to N. 20° E. and dips 55° to 80° east [Nash and Lehrman, 1975 (11)] with foliation parallel to bedding [Fleshman and Dodd, 1982 (4)]. Amphibolite sills that conform to the bedding planes appear to be about the same age [Nash and Lehrman, 1975 (11)].

A porphyritic quartz monzonite intrusion of Late Cretaceous age crops out along the west side of the mine [Fleshman and Dodd, 1982 (4)] and forms the west high-wall and ridge of pit 4 and part of the west highwall of pit 3. In the northwest corner, large xenoliths of phyllite are found. It is unclear whether the intrusive once cropped out between pits 3 and 4 because the area is now covered by waste rock.

Dikes and sills of aplite cut or grade into the quartz monzonite [Ludwig, Nash, and Naeser, 1981 (8)]. During the Eocene, all units were intruded by andesite-dacite feeder dikes of the Sanpoil volcanics [Fleshman and Dodd, 1982 (4)]. Thickness of alluvium ranges from nearly non-existent on some mine roads to several tens of meters in ancestral drainages.

The general trend of the structural features in the area is north-northeast and south-southwest; these features include fractures, the Midnite mineral trend, and the dikes and sills. The mine is on the west limb of a broad north-east-southwest-striking structural feature—the Deer Trail anticlinorium [Robbins, 1978 (18)]. The beds appear to be overturned to the east; in the mine area, they dip to the east, and small drag folds are locally present although they are not found near the mine [Ludwig, Nash, and Naeser, 1981 (8)]. Most of the small faults and shear zones in the mine area trend northeast-southwest, dip steeply (from 50° to 70° west), and extend for only a short

distance before ending. Clay minerals are associated with these features within the quartz monzonite [Fleshman and Dodd, 1982 (4)]. One fault near pit 2 appears to have displaced a calc-silicate block but did not offset the ore zone [Nash and Lehrman, 1975 (11)]. The ages of the small faults vary considerably; some are truncated by the intrusion and others deform dikes of the Sanpoil volcanics [Ludwig, Nash, and Naeser, 1981 (8)]. A northwest-southeast-trending normal fault zone in pit 3 offsets a major andesite-dacite dike and a member of the Togo Formation by 18 m (60 ft) [Nash, 1977 (10)].

The contact between the quartz monzonite and the metasediments appears to run north-south from the middle of pit 4 through pit 3 near the west wall. The contact

is very irregular, and tabular mineralized zones are found in the troughs of the monzonite [Ludwig, Nash, and Naeser, 1981 (8)]. Ore bodies are up to 18 m (60 ft) wide, 366 m (1,200 ft) long, 46 m (150 ft) thick, and 4.6 to 91 m (15 to 300 ft) below the surface. These ore bodies were emplaced in a series of deposition and enrichment stages [Fleshman and Dodd, 1982 (4); Milne, 1979 (9)]. Oxidized uranium minerals—autunite and metaautunite—occur above the water table. Reduced primary uranium minerals—uraninite and coffinite—are found in the deep ore bodies below the water table. Pyrite and marcasite appear to be associated with the latter minerals. Several other sulfide minerals are also present in minor amounts: pyrrhotite, molybdenite, chalcopyrite, sphalerite, and galena.

ACKNOWLEDGMENTS

The authors would like to thank John A. Riley, consultant, Post Falls, ID, for designing the initial monitoring system and supervising the installation of the sampling wells. Discussions with Riley also provided insight regarding possible flow path models.

Also, the authors would like to thank Charles N. Alpers, geochemist, U.S. Geological Survey (USGS), for his assistance in the use of the WATEQ4F and BALANCE computer programs as part of an interagency agreement.

METHODS

FIELD

Fifteen monitoring wells at 7 locations and 14 surface locations were monitored monthly from December 1989 to April 1992 (fig. 1). These sites were chosen to allow documentation of the full range of water elevation and quality at the mine. For example, well 89-6 was placed high on the ridge at the northern edge of the Hillside Spoils to sample uncontaminated water recharging the minesite, while several surface seeps on and below the South Spoils area are being sampled to collect water being contaminated within the mine.

During the selection of the field sampling locations, it was decided to concentrate data collection on the eastern side of the mine. This allowed more monitoring wells to be installed in that area and increased the probability of gathering sufficient data from a single area to understand the hydrogeology and geochemistry.

The 15 monitoring wells were drilled between August 8 and October 16, 1989, according to methods required for resource protection wells in Washington State [1971 (24)]. Figure 5 is a set of sketches of the completion details, including well depth; elevation; generalized lithology; and screened, sand-packed, and bentonite-sealed intervals. The deepest completion at each location was in the quartz monzonite intrusive. Holes with an inside diameter of 20.3 cm (8 in) were drilled using an air-rotary drilling rig. Steel casing was driven as needed to stabilize the hole

during drilling. After completion, the steel casing was pulled, leaving only 3 to 6 m (10 to 20 ft) of permanent 20.3-cm (8-in) steel casing at the top of the well.

All monitoring wells were constructed with 5-cm (2-in) threaded polyvinyl chloride casing and 5-cm- (2-in-) diam factory-slotted screens. The screened sections were 1.5 m (5 ft) long, and a 1.5- or 3-m- (5- or 10-ft-) long blank sump was installed below the screen. A threaded end cap was placed at the bottom of each casing string. One, two, or three monitoring wells were installed inside the 20.3-cm (8-in) drill hole, depending on the number of intervals that contained water for sampling and the intended purpose for the hole. Clean silica sand was poured into the drilled hole in the interval around the screened section.

Benseal,⁶ a bentonite sealing material containing additives that cause the bentonite to set to the consistency of gelatin within 20 min of mixing, was pumped into the hole with a tremie line to seal the intervals between the screened sections. Either Benseal sealing material or a viscous bentonite slurry was then used to seal the well from the top of the shallowest sand pack to the surface. The surface seal was topped off if any settling occurred.

Wells were pumped using air-driven submersible bladder pumps. Air pressure was used to inflate and deflate

⁶Reference to specific products does not imply endorsement by the U.S. Bureau of Mines.

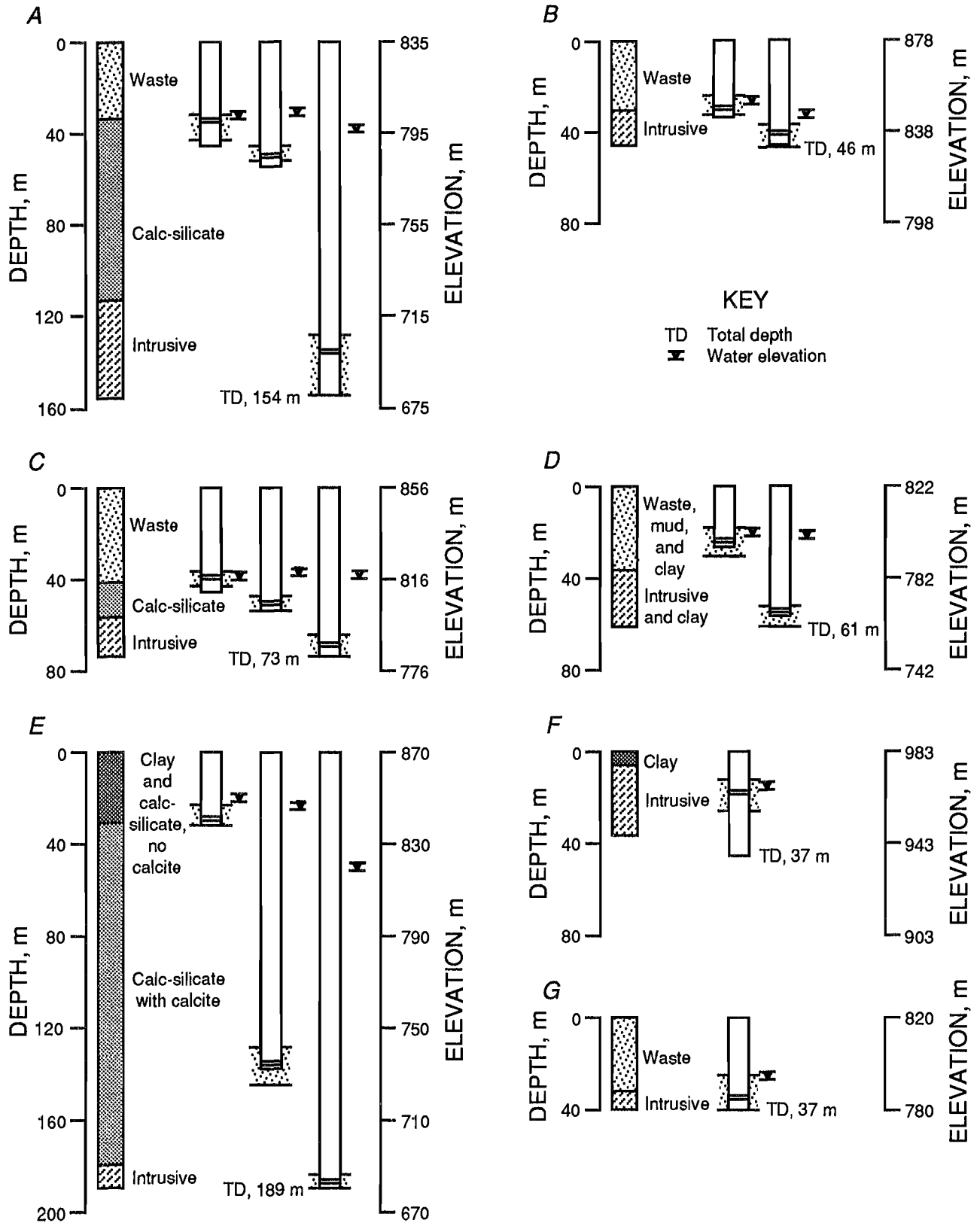


Figure 5.—Details of well completion at seven sampling locations. A, Well 89-1; B, well 89-2; C, well 89-3; D, well 89-4; E, well 89-5; F, well 89-6; G, well 89-7.

a bladder alternately and thereby pump water to the surface. In this way, the water sample did not contact atmospheric oxygen until after the field variables were measured. Changes in pH, oxidation-reduction potential (Eh), and alkalinity were minimized, and the chemical composition of the water sample was preserved.

Several surface locations and wells can become inaccessible in the winter or during extremely wet weather, while other surface locations and two shallow wells dry up in the summer. When this occurred, no readings were obtained from that location.

Measurements of specific conductance, temperature, pH, Eh, and dissolved oxygen (DO) content were made in the field using a flowthrough cell. The probes were calibrated according to the manufacturer's instructions and were replaced when their operation was sluggish or erratic. The instrument manufacturer claims accuracy as specified in table 1.

Table 1.—Instrument calibration accuracy

<i>Condition</i>	<i>Precision</i>
Temperature	±0.4° C.
Specific conductance	±3 pct of full scale from 0 to 2,000 mS/m.
pH	Subject to calibration.
Eh	±2 pct of reading.
DO	+1 pct of full scale at calibration temperature.

Samples were obtained in accordance with standard U.S. Environmental Protection Agency (EPA) sampling procedures [EPA, 1983 (23)] and transported to the analytical laboratory at SRC for chemical analyses of major cations, anions, and trace constituents.

The sampling procedure consisted of measuring the depth-to-standing-water level at each well. Then each well was pumped to remove at least three volumes of water standing in the casing while passing the water through a flowthrough chamber containing probes for measuring temperature, pH, Eh, and specific conductance until these measurements stabilized. The alkalinity was measured within 5 min of sample collection using a digital titrator, then the DO readings were taken. The water was vacuum filtered through 0.45- μ m filters and collected in two polyethylene 70-mL bottles after the bottles and caps were rinsed twice with the filtered water. One was left unacidified for anion analysis; the second was acidified with nitric acid for cation analysis.

As of April 1992, 28 months (November 30, 1989, through April 1, 1992) of readings and samples have been collected from the field; the samples have been analyzed, and the data have been entered into computer files.

LABORATORY

Cation analyses were performed on an ARL model 34000, inductively coupled plasma-atomic emission spectrometer (ICP-AES). This is a simultaneous instrument capable of analyzing up to 24 elements per sample. Samples from the first 7 field collections were analyzed for all 24 elements. The analytical method was then shortened to remove elements that had measured values below the detection limit for the instrument. These elements and their detection limits, in milligrams per liter, were arsenic, <1.5; selenium, <0.3; tin, <0.6; mercury, <0.4; and chromium, <0.02.

The ICP-AES was operated following EPA guidelines [EPA, 1983 (23)]. Calibration solutions were prepared by serial dilution of stock standard solutions obtained from SPEX Industries, Inc., Edison, NJ. In addition to the check standard solutions specified by EPA, a large quantity of one of the mine water samples containing high concentrations of metal ions was collected and stabilized, and used as an additional control sample during the analyses. The long-term precision of the analyses was ±5 pct for those elements whose concentrations were >10 times the detection limit of the ICP-AES. Those elements whose concentrations were consistently <10 times the detection limit exhibited variations of up to ±20 pct.

Anion analyses were performed using a Dionex Series 4000i gradient ion chromatograph. The column used for this sample set, the AS4A, has the capability to detect 10 anions. The first few sample sets were analyzed for all possible anions, but the analytical procedure was shortened once the anions actually present had been identified. Routine analyses were performed for chloride, nitrate, and sulfate.

Quality control for anion analysis was similar to that for cation analysis and also followed EPA guidelines [EPA, 1983 (23)]. The instrument was calibrated daily using a series of standards prepared from stock, single-ion standards obtained from Environmental Resource Associates, Arvada, CO. The eluant was prepared from Baker Analyzed, reagent-grade, sodium carbonate crystals and sodium bicarbonate powder to concentrations of 2.8 and 2.7 mM, respectively. An eluant flow rate of 2.0 mL/min was used.

DATA COLLECTION

GROUND WATER ELEVATIONS AND FLOW PATHS

Water elevations in the monitoring wells varied from 967 m (3,171 ft) above sea level in well 89-6, located at the north end of the Hillside Spoils, to 792 m (2,600 ft) in well 89-7, located about 60 m (200 ft) north of the face of the South Spoils. Water elevations were different in those wells with multiple completions, indicating that the bentonite seals between completions successfully isolated the screened zones from each other. This isolation ensures that the samples collected for water quality monitoring are from one geologic formation and are not a mixture of water from several formations.

Ground water flow at wells with multiple completions is, in most wells, downward, which was expected because the mine lies in the recharge portion of the flow path [Freeze and Cherry, 1979 (5)]. The direction of ground water flow implies that contaminants could migrate down, but, in fact, only limited downward migration of contaminants occurred at this site.

Discharge from surface sampling locations was measured whenever possible. The volumetric discharge rate can be multiplied by the concentrations of elements of interest to calculate the mass load of a metal being discharged from a given site. The seasonal variation in discharge (or lack thereof) is an indication of the length of flow path that feeds the discharge point.

The direction of ground water flow primarily follows the local topography, from north-northwest to south-southeast. Contours of ground water elevations are presented in figure 6. The contour lines indicate that water flows from the ridges at the north end of the site toward the spoils piles and surface drainages at the south end of the site. The water elevation at well 89-5 was between 6 and 40 m (20 and 130 ft) higher than the water elevation in pit 3, depending on the depth of the completion zone and the season of the year. Therefore, water from pit 3 cannot migrate in the direction of the East Drainage, but must go in a southerly direction. The elevation of water in pit 3 was approximately 15 m (48 ft) higher than the elevation of Boyd Seep, suggesting that one of the sources for Boyd Seep might be pit 3. A more detailed discussion of this possibility is presented in the section "Presentation and Interpretation of Data." The water elevation in well 89-3M was 4 m (14 ft) higher in June 1992 than the water elevation in pit 3.

Detailed information on the ground water flow path is still lacking in some areas. Possible flow paths have been developed for East Drainage, since most of the initial monitoring wells were placed in that area. The flow path in the West Drainage area will require additional well installations to resolve questions about contaminant sources and migration.

COMPUTER MODELING METHODS

Analytical data from field and laboratory measurements were entered into computer models to assist in determining the geochemical characteristics of the water samples. Modeling was also used to determine the changes in water chemistry that must occur along a proposed flow path in order for the water quality characteristics at one location to evolve into the characteristics at another location. The analysis of evolution of water chemistry along a proposed flow path can substantiate or refute the existence of a path between sampling locations. Typically, the models cannot prove the existence of a flow path. They can, however, provide convincing evidence against the existence of the proposed path.

The two computer programs used were WATEQ4F [Ball, Nordstrom, and Zachman, 1987 (3)] and BALANCE [Parkhurst, Plummer, and Thorstenson, 1982 (16)]. WATEQ4F is a computational device that uses equilibrium equations and constants from a thermodynamic data base to identify and quantify the dissolved species in a water sample. It then uses that information to determine whether the water is saturated with respect to any of >500 mineral phases.

WATEQ4F expresses the degree of mineral saturation in a sample using a calculated value called the saturation index. The saturation index is defined as the log (base 10) of the ratio of the observed ion activity product (IAP) to the thermodynamic solubility product constant (K_{sp}). The sample is saturated if $IAP = K_{sp}$; it is undersaturated if $IAP < K_{sp}$; and it is supersaturated if $IAP > K_{sp}$. WATEQ4F calculates the \log_{10} of this ratio to facilitate the evaluation of the saturation index in the printout. Thus, the sample is at equilibrium if saturation index = 0, undersaturated if saturation index < 0, and supersaturated if saturation index > 0.

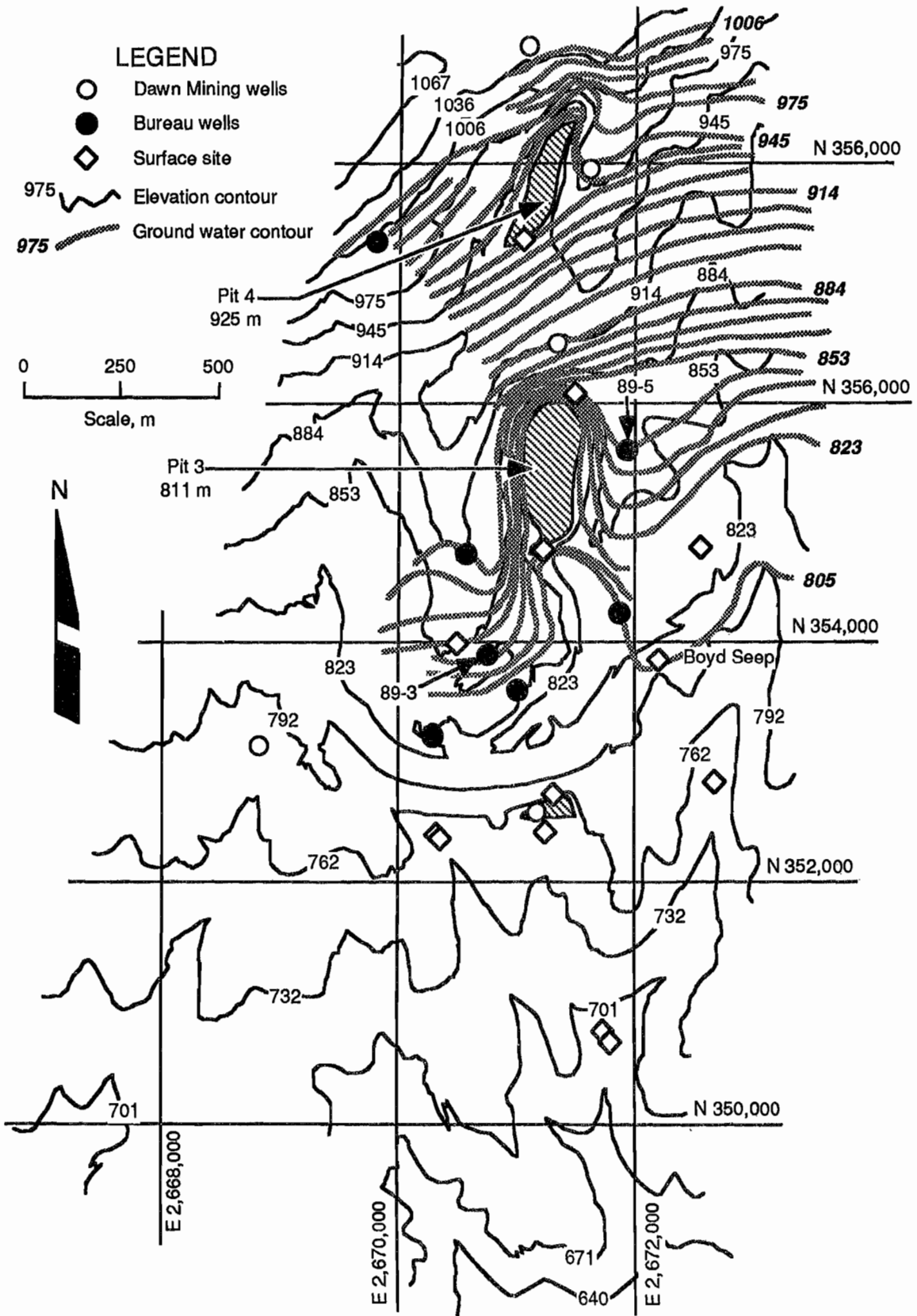


Figure 6.—Ground water elevation contours.

BALANCE solves a set of linear equations based on the observed molality of two or three water samples, dissolution or precipitation of mineral phases, possible ion exchange reactions, and the gases known to be present. BALANCE does not utilize any thermodynamic data; it is strictly a means of setting up and solving a matrix of linear equations based on mass balance. The equations are derived from dissolution reactions of the mineral phases entered into the program. Table 2 presents mineral and gas phases that have been identified by previous investigators at the Midnite Mine. The calculation balances the mass in the chemical reactions necessary to produce water having one set of measured concentrations of constituents from one or two sources of water with measured concentrations from a different set, using mineral phases as needed. A positive sign on the mineral in the output indicates that the mineral is dissolving, whereas a negative sign indicates that the mineral is precipitating or degassing.

Table 2.—Possible minerals and gases used as input for BALANCE program

Phase	Formula
Albite	NaAlSi ₃ O ₈
Anorthite	CaAl ₂ Si ₂ O ₈
Calcite	CaCO ₃
Ca-montmorillonite	Ca _{0.25} Si ₄ Al _{1.5} Mg _{0.5} O ₁₀ (OH) ₂
Carbon (organic)	"CH ₂ O"
Carbon dioxide gas	CO ₂
Diopside	CaMgSi ₂ O ₆
Dolomite	CaMg(CO ₃) ₂
Gibbsite	Al(OH) ₃
Goethite	FeOOH
Gypsum	CaSO ₄ •2H ₂ O
Jarosite	KFe ₃ (OH) ₆ (SO ₄) ₂
Jurbanite	Al(OH)SO ₄ •5H ₂ O
Kaolinite	Al ₂ Si ₂ O ₅ (OH) ₄
K-feldspar	KAlSi ₃ O ₈
K-mica	KAl ₃ Si ₃ O ₁₀ (OH) ₂
Manganite	MnOOH
Oxygen gas	O ₂
Pyrolusite	MnO ₂
Silica	SiO ₂
Sphalerite	ZnS

Sign conventions and solid phase generalizations are used in BALANCE. During input, an optional algebraic sign can be used in the mineral and gas input data table to constrain a solid phase to only dissolve (+) or only precipitate (-). A solid phase can do either if no sign is used. Algebraic signs are shown in the output to indicate if a mineral is constrained to be consumed (+) or precipitated (-). Only the stoichiometric ratios of elements in a solid phase, not the mineralogy, are considered in BALANCE. Thus, ferrihydrite [Fe(OH)₃] and goethite [FeO(OH)] are equivalent minerals in BALANCE because they both contain one iron atom with a +3 oxidation number. Since acid water production involves oxidation-reduction reactions, it is necessary to conserve electrons when balancing the chemical equations. BALANCE uses a convention that defines a redox state for a solution as

$$RS = \sum_{i=1}^I m_i v_i \quad (1)$$

where RS is the redox state of the solution, I is the total number of species, m_i is the molality of the i^{th} aqueous species, and v_i is the valence of the i^{th} species. The reader is referred to the USGS documentation of WATEQ4F and BALANCE for complete descriptions of the models and variables [Ball and Nordstrom, 1991 (2); Ball, Nordstrom, and Zachman, 1987 (3); Parkhurst, Plummer, and Thorstenson, 1982 (16); Plummer, Prestemon, and Parkhurst, 1991 (17)].

In most cases, more than one solution is produced from input to the BALANCE program, so these solutions are nonunique. Acceptance or rejection of possible solutions is based on knowledge of the saturation state of the water samples as calculated by WATEQ4F, information on initial mineralogy and likely secondary minerals, plus field observations. For example, it is not realistic to expect a mineral such as quartz to be precipitated from a solution because silica is generally limited by saturation with amorphous silica, which is considerably more soluble than quartz. Alternately, if the saturation index of a particular mineral phase (as calculated by WATEQ4F) is <0, then that mineral phase cannot precipitate from solution, and any model produced by BALANCE that includes precipitation of that mineral phase should be rejected by the investigator.

PRESENTATION AND INTERPRETATION OF DATA

The Midnite Mine is a dynamic system moving toward equilibrium. Large variations in water quality exist at the site and reflect differences in the types and extent of chemical reactions that are taking place. In the following

discussion, the water quality data from specific sampling locations will be used to discuss the chemistry, after which differences in the chemistry will be used to evaluate possible flow paths on the site.

Most of the data in table 3 were produced from analyses of samples collected in May 1991 (sample collection 18). Exceptions are data from the South Dump Seep (sample collection 17), rainwater, and data collected from well 89-6, which are averages. The use of data collected during a specific time period allowed water

quality at different sampling locations to be compared at a particular moment in time. Observed changes in constituents over time at selected sampling locations are also presented. Selected data from the computer models are given in tables A-1 through A-45 in the appendix.

Table 3.—Water quality data

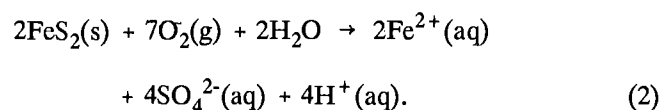
Location	Specific conductance, mS/m	pH	Eh, mV	SO ₄ , mg/L	Alkalinity, mg/L as HCO ₃	DO, mg/L	Element, mg/L		
							Al	Ca	Fe
Well 89-6	4.0	5.8	473	6.4	41	6.4	<0.3	7.5	0.02
Rainwater	.69	5.6	NR	.57	.0044	NR	NR	.16	NR
Well 89-5D	21.8	7.0	401	10.1	177	4.3	<.3	30	.18
Blood Pool	168.0	3.3	619	2,470	0	8.9	89	441	17
Pit 3	256.0	4.3	440	2,450	0	9.9	50	397	1.2
Boyd Seep	158.0	4.2	434	3,480	0	10.2	78	473	.24
Well 89-1S	83.0	7.3	455	224	342	6.4	<.3	12	.05
Well 89-1M	46.0	7.2	445	119	262	6.1	<.3	82	.12
Pit 4	59.6	8.2	491	394	55	10.6	<.3	117	.03
Pit 3 seep	70.7	7.5	419	2,452	85	9.8	<.3	200	.06
Sis Pool	754.0	2.7	473	17,370	0	NR	1,560	408	141
Well 89-3M	799.0	5.4	403	10,070	506	1.4	22	445	1,560
Well 89-3D	68.0	6.7	465	342	140	3.5	<.3	108	.03
Well 89-4S	4.40	4.40	502	5,880	0	4.6	191	477	33
South Spoils Seep	292.0	3.3	431	8,890	0	NR	464	439	2.4
East Drainage									
Control	33.0	7.8	471	39.2	262	9.8	<.3	76	.03
East Drainage 11.	68.0	8.1	481	319	268	10.3	<.3	159	.05
West Drainage									
Control	159.0	4.3	413	2,690	0	4.6	14	493	.10
West Drainage	157.0	4.4	389	2,635	0	8.7	20	473	.27
Well 89-7	60.8	6.1	422	237	104	1.5	<.3	87	.01

Location	Element, mg/L—Continued							
	K	Mg	Mn	Na	Ni	Sj	U	Zn
Well 89-6	<1.5	2.6	0.007	4.1	<0.03	11	<1	<0.04
Rainwater	.052	.025	NR	.18	NR	NR	NR	NR
Well 89-5D	3	4.0	.15	30	<.03	14	<1	.13
Blood Pool	5	137	31	22	1.3	23	6	1.2
Pit 3	4	222	95	54	2.8	11	21	3.7
Boyd Seep	12	358	82	65	3.2	15	18	5.3
Well 89-1S	3	2.7	.07	232	<.03	8.8	<1	<.04
Well 89-1M	4	20	.03	12	<.03	22	<1	<.04
Pit 4	3	29	.40	17	.05	9.2	3	<.04
Pit 3 seep	4	84	17	25	.06	13	2	.09
Sis Pool	2	1,260	601	14	25	49	45	34
Well 89-3M	7	1,290	942	51	29	25	16	21
Well 89-3D	3	31	16	21	.03	7.1	1	.15
Well 89-4S	7	642	377	46	11	15	48	11
South Spoils Seep	4	829	503	35	16	28	116	23
East Drainage								
Control	2	13	.019	6.3	<.03	23	<1	<.04
East Drainage 11.	4	37	.16	11	<.03	24	<1	<.04
West Drainage								
Control	8	336	55	43	1.6	19	4	1.5
West Drainage	7	309	49	41	1.3	18	6	1.3
Well 89-7	2	25	.29	14	<.03	20	<1	.08

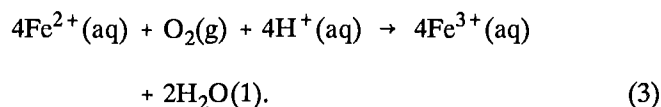
NR Not reported.

There are two chemical processes that must be considered when evaluating the hydrochemistry of the Midnite Mine: acid water production caused by oxidation of minerals containing reduced sulfur (primarily pyrite) and reaction of the acid water with other minerals. A comprehensive review of the inorganic and microbial mechanisms of pyrite oxidation is presented by Steffan, Robertson, and Kirsten, Inc. [1988 (21)]. Pyrite is oxidized when it comes into contact with air and water, leading to the formation of oxidized iron compounds and sulfuric acid.

Oxidation occurs in three major steps. The first step is the oxidation of pyrite by molecular oxygen. Pyrite has two oxidizable species, ferrous ion and sulfidic sulfur. During the initial solubilization, only the sulfur species is oxidized, and the iron is dissolved in the ferrous state (Fe^{2+}) [Lowson, 1982 (7)], as shown in equation 2.

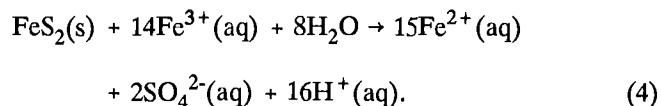


The second reaction is the oxidation of the Fe^{2+} to the ferric ion (Fe^{3+}) by molecular oxygen, which can be catalyzed by the bacteria *Thiobacillus ferrooxidans*.



Above a pH of 4, the reactions shown in equations 2 and 3 dominate the kinetics of pyrite oxidation with molecular oxygen as the oxidant [Nordstrom, 1982 (13)]. Combining these reactions show that 15 mol of molecular oxygen is required for every 4 mol of pyrite oxidized, or a ratio of 3.75 mol O_2 to 1 mol FeS_2 .

The third reaction involves the oxidation of pyrite by Fe^{3+} .



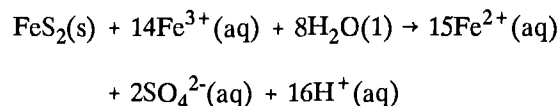
As the pH falls below 4 and the solubility of Fe^{3+} increases, Fe^{3+} becomes the dominant oxidant [Nordstrom, 1982 (13)].

The overall stoichiometric equation that describes the oxidation of pyrite is given by a modification of equation 4 [Nordstrom, Jenne, and Ball, 1979 (14)].

Regenerated (oxidized) by

Thiobacillus ferrooxidans

↓ ↑



↓

hydrolysis and precipitation of Fe^{3+}

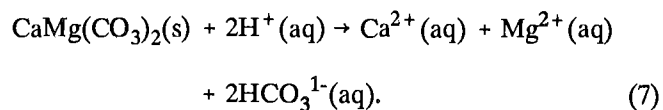
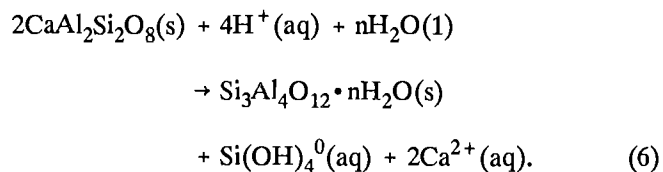
↓

$\text{Fe}(\text{OH})_3$ amorphous "yellow boy," $\text{FeO}(\text{OH})$ goethite,

or $\text{KFe}_3(\text{OH})_6(\text{SO}_4)_2$ jarosite. (5)

As shown in equation 5, the pyrite is oxidized by Fe^{3+} . The Fe^{2+} is oxidized through metabolic pathways of the bacterium with oxygen as the electron acceptor according to equation 3. Under aerobic conditions during pyrite oxidation, the pH of the water decreases and high concentrations of iron and sulfate ions are produced; these conditions are typical indicators of acid water.

However, at many of the sampling locations at the Midnite Mine, the acid water reacts with other minerals, raising the pH and increasing the concentrations of sodium, calcium, and magnesium ions. For example, the reactions of anorthite ($\text{CaAl}_2\text{Si}_2\text{O}_8$) or dolomite [$\text{CaMg}(\text{CO}_3)_2$] to yield allophane ($\text{Si}_3\text{Al}_4\text{O}_{12} \cdot n\text{H}_2\text{O}$) as follows [Sposito, 1989 (20)]:



Therefore, elevated concentrations of calcium and magnesium ions become indicators of neutralization reactions.

At low pH levels, elevated concentrations of aluminum, manganese, zinc, and uranium ions are found in the water, but as pH increases as a result of neutralization reactions, concentrations of aluminum and manganese ions are controlled by precipitation of secondary minerals, as shown for aluminum ions in equation 6. Therefore, zinc and uranium are used to indicate the movement of toxic metals in water having a near-neutral pH.

RAINWATER

It would be helpful if water quality data were available on precipitation at the site; however, the only data available are those on quantity, not quality. On the assumption that precipitation across northeastern Washington has similar characteristics, data were obtained for a site approximately 32 km (20 miles) northeast of the study area, at Sullivan Lake [National Resource Ecology Laboratory, 1987 (12)]. Table 3 provides averages of measurements made on samples collected for 19 days between January and July 1987. As would be expected, the average specific conductance was low, which indicates low amounts of dissolved solids, and pH was close to the equilibrium value with carbon dioxide in the atmosphere.

WELL 89-6

Well 89-6 is a source of uncontaminated water in the quartz monzonite intrusive (fig. 5F). The well lies at the top of a ridge on the northwest flank of the minesite; water from this well represents recharge water shortly after it has entered the intrusive. Table 3 presents an average of values from water collected in August, September, and October 1990. Any individual sample typically gave a charge balance >10 pct, where the charge balance was calculated by dividing the difference between the sum of the cation species and the sum of the anion species by the average of the sums and then converting them to percentages. The charge balance discrepancy appears to be caused by fluctuations in field alkalinity. Because no other temporal variations have been observed for other water quality measurements at well 89-6, an average was calculated that gave a better charge balance (<10 pct) and better represented water quality. The results show that water from this well is of magnesium-calcium bicarbonate type, highly oxygenated, nearly in equilibrium with atmospheric carbon dioxide, and contains low concentrations of total dissolved solids.

When the averages were entered into WATEQ4F, the output (table A-1) indicated that the water was undersaturated for most of the primary minerals at the minesite, including the major feldspars and diopside. The only

minerals with saturation indices near 1 or >1 were montmorillonite, which is a secondary mineral stable in neutral soils, some iron-bearing minerals, and quartz. The water contained low concentrations of iron as Fe^{3+} ; these concentrations appear to be controlled by ferrihydrite solubility. Silica concentrations are usually controlled by amorphous silica, and in this sample, amorphous silica had a negative saturation index. The concentration values indicate kinetic control of silica instead of equilibrium control.

COMPARISON OF RAINWATER AND WATER FROM WELL 89-6

Using the rainwater data as representative of precipitation at the Midnite Mine, the BALANCE program was run to investigate the changes that would have to take place to form the water at well 89-6. Using minerals consistent with the saturation indices computed by WATEQ4F, two models were produced that satisfied the constraints of the mass balance (tables A-2 to A-4).

In both models, albite, diopside, K-mica, and calcite are dissolved, which increases specific conductance. Pyrite is oxidized, producing increased concentrations of sulfate, and goethite is precipitated, which maintains low iron concentrations consistent with Eh and pH measurements.

The only difference in the models is the source of the carbon needed to produce the increase in alkalinity measured at well 89-6. Because of constraints placed on the dissolution of carbonate minerals by calcium and magnesium concentrations, an additional source of carbon must exist. In one model, the source is carbon dioxide gas. This condition would be reasonable because the water was infiltrating through the root zone where carbon dioxide levels are significantly higher than in the atmosphere. The other model uses oxidation of organic carbon species to produce the bicarbonate ion. This is also plausible, since the water was infiltrating through a plant cover and a developed surface horizon in the soil. No determinations of organic carbon have been made to resolve the difference in the models. For the purposes of this report, the source of the bicarbonate carbon was not deemed critical.

WELL 89-5D

The water in well 89-5D is representative of the types of changes that are typical in an uncontaminated flow path. Water quality data are given in table 3, and the WATEQ4F saturation indices are given in table A-1.

At well 89-5D, the water is still unsaturated with respect to the primary minerals anorthite, calcite, and diopside. Silica concentrations are approaching saturation for amorphous silica. Aluminum appears to be controlled by a substance several orders of magnitude more soluble than

the crystalline gibbsite listed in the table. Since aluminum was below the detection limit of the ICP-AES (0.3 mg/L), a concentration of 0.1 mg/L was entered into the program to allow inclusion of aluminum species in the calculations. It appears that this value is slightly high, and equilibrium control is probably maintained by amorphous aluminum hydroxide. Iron concentrations are supersaturated with respect to ferrihydrite and goethite. Because the aqueous iron species are primarily $\text{Fe}(\text{OH})^{2+}$ and $\text{Fe}(\text{OH})_3^0$ as calculated by WATEQ4F, it is possible that the filters used in the field, with a pore diameter of 0.45 μm , allowed some of the suspended iron species to pass through.

BALANCE was run using the concentrations from well 89-6 as initial concentrations and those from well 89-5D as final concentrations to see what changes could be expected to take place along a flow path through the quartz monzonite intrusive in the absence of mining (tables A-5 to A-7). As would be expected from comparing the saturation indices, the model indicates that albite, calcite, and diopside dissolve along the proposed flow path. The dissolution of calcite is consistent with the increase in pH, from 5.8 to 7.0. Silica and gibbsite are formed as secondary minerals. A small amount of oxygen gas is consumed, which is consistent with the decrease in measured DO and Eh (table 3). No measurable quantities of toxic metals, such as uranium, zinc, or nickel, were found in well 89-6. This indicates that outside the mineralized zone of the ore body, no detectable quantities of toxic metals are produced down a flow path. Only small increases of soluble salts would be expected.

BLOOD POOL

A small surface pond, named Blood Pool by site workers (designated BP in figure 2) and located downhill from the water treatment plant, is a good example of acid mine drainage (table 3). The pond received its name because of its blood red color. The pH of the water is low, Eh is oxidizing, and sulfate, iron, and other metal concentrations are high. The elevated iron and sulfate concentrations are the direct result of the oxidation of pyrite or another iron-sulfide mineral such as marcasite (see equations 2-5).

Data from the analysis of water from Blood Pool were entered into WATEQ4F to evaluate aqueous speciation of ions and to identify possible solid phases that might be controlling solution concentrations (table A-8). The predominant iron solution species are Fe^{2+} and FeSO_4^0 . At these low pH and high sulfate levels, the solubility of iron is apparently controlled by jarosite, which is a potassium ferric sulfate formed in acidic soils and as a result of acid mine drainage [Nordstrom, 1982 (13)]. As pyrite is oxidized, high concentrations of hydrogen ions are produced. This makes the solution very corrosive and able to dissolve other minerals in the rock matrix, resulting in high

concentrations of calcium, magnesium, and aluminum [Nordstrom and Potter, 1977 (15)].

The concentration of calcium ion seems to be controlled by the solubility of gypsum. As the concentration of sulfate increases because of acid water formation, the concentration of calcium ion reaches a maximum limited by gypsum solubility. Aluminum ion concentration is apparently controlled by jurbanite solubility. At the low pH found in these samples, the solution is undersaturated for allophane and for crystalline gibbsite.

Silicon ions are removed from the primary minerals and secondary minerals are produced. At low pH levels, the solubility of silica is controlled by amorphous silica [Wilding, Smeck, and Drees, 1977 (25)]. The concentrations of metal species such as manganese, nickel, and zinc are controlled by the availability of mineral phases containing these elements and the kinetics of dissolution. At Blood Pool, the saturation indices of all toxic-metal-bearing minerals are large negative numbers, indicating undersaturation.

The water at Blood Pool is seasonal, suggesting that the water has a short flow path through the surface waste rock uphill from the seep. To evaluate this possibility, BALANCE was used to compare water along such a flow path. The input parameters are given in tables A-9 to A-11, along with possible solutions to the mass balance equations. The amount of precipitation and infiltration determines the amount of water that surfaces at the pool. Water entering the waste rock was assumed to be similar to water found at well 89-6. Diopside, K-feldspar, albite, anorthite, and calcite are the major mineral phases found in the area [Nash, 1977 (10)]. The other mineral phases were selected on the basis of the values of the saturation indices calculated by the WATEQ4F program.

Several models were generated that satisfied the mass balance constraints. The major differences in the models (table A-11, models 5A-5D) are in the formation of gibbsite, jurbanite, jarosite, and goethite, and the relative amounts of anorthite, K-feldspar, and calcite dissolved. To provide uniformity in the models run for various locations, goethite was used in the input as a possible secondary mineral for reducing the iron levels in solution. It made no difference in the mass balance equations which of the iron oxyhydroxides (goethite or ferrihydrite) were used for this evaluation.

In model 5A, the iron produced from the oxidation of pyrite is removed from solution as goethite. WATEQ4F shows the water at Blood Pool to be supersaturated with respect to goethite by about four orders of magnitude, but undersaturated with respect to ferrihydrite. The amount of K-feldspar consumed is low; the dissolution brings small quantities of potassium into solution.

The second model (5B) incorporates the dissolution of a larger amount of K-feldspar. The increased mass of

potassium is removed from solution as jarosite. Since the saturation index for jarosite is slightly positive, this is a plausible model considering the pH and sulfate concentrations at Blood Pool. Also, less goethite forms because Fe^{3+} is removed during the formation of jarosite.

Models 5A and 5B both show the formation of amorphous silica, which is consistent with the saturation index calculated by WATEQ4F. The rock-forming silicates are undersaturated and may be dissolving, depending on contact time and the rates of the dissolution reactions. Both models show the dissolution of calcite, which is consistent with the measured pH and the increasing concentrations of calcium along the flow path. Neither model shows precipitation of gypsum as an option for controlling the calcium concentration as calculated by WATEQ4F. This may indicate that the models are conservative and that greater amounts of primary minerals are dissolving, but the ratios are consistent with this mass balance. The oxygen gas-pyrite ratio was 3.70, which is very close to the theoretical value of 3.75 found in the summation of the oxygen consumed in equations 2 and 3.

Two other models show both increased amounts of primary minerals being dissolved and control of aluminum concentrations by jurbanite (table A-11, models 5C and 5D). In model 5C, iron is controlled with jarosite similar to model 5B. Model 5D shows the largest quantity of minerals being dissolved, including anorthite; this model also requires larger quantities of secondary minerals to be formed, with jarosite controlling solution concentrations of Fe^{3+} and jurbanite controlling concentrations of aluminum. On the basis of the saturation indices calculated by WATEQ4F, models 5C and 5D probably best describe the chemistry of Blood Pool.

To summarize, acid water is produced in the pyrite-containing waste rock uphill from Blood Pool. As the water migrates downslope, it dissolves the primary minerals, producing high concentrations of ions in solution. The water emerges at the northwest wall of the basin and forms a pool. Evaporation causes the concentrations of dissolved species to exceed the solubility levels of minerals such as jurbanite, jarosite, and amorphous silica. Evaluation of the water quality data using the computer programs, along with field observations, leads to the conclusion that acid water is produced as infiltration water moves through the unsaturated zone at the minesite.

BOYD SEEP

Temporal Variations in Water Quality

Another seep on the east side of the mine, known as the Boyd Seep, produces acidic water and elevated concentrations of toxic metals (table 3). Figure 7 presents seasonal fluctuations in amount of discharge and changes

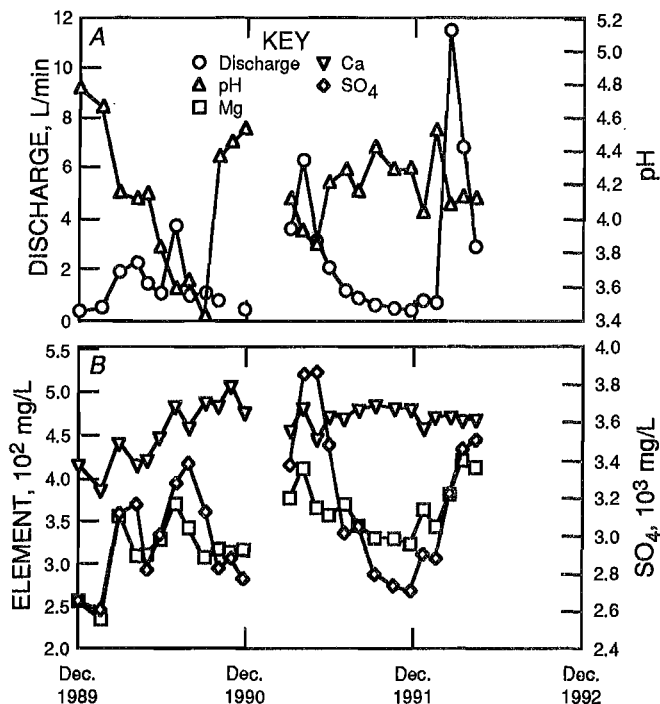


Figure 7.—Temporal variations in ground water quality at Boyd Seep. A, Amount of flow and pH; B, calcium, magnesium, and sulfate.

in pH, and calcium, magnesium, and sulfate concentrations. Contaminant levels increased during wet periods. As flow in the system increased, concentrations of ions also increased and pH decreased. This coupling indicates that chemical reaction products were being flushed from reaction sites in the waste rock and brought to the surface. It was speculated that pyrite oxidation and acid water formation occur during the dry seasons, and soluble sulfate salts build up in the pore spaces in the sediments and the fractures in the rocks. The movement of water through the sediments during the wet period dissolves the salts and increases their concentrations in ground water in the spring.

Calcium concentrations were maintained at fairly constant levels after midsummer 1990. The saturation index for gypsum was near zero, showing saturation (table A-12). After the system was flushed and concentrations of other ions decreased, concentrations of calcium remained roughly constant (refer to figure 7, July 1990 to December 1990). The gypsum that precipitated when sulfate concentrations were highest began to be dissolved, maintaining a saturated solution. The concentration of sulfate would have decreased even more if it had not been for the dissolution of gypsum. This mechanism is distorted by a continual increase in concentrations of reaction products, as seen in figure 7.

The quantities of several toxic contaminants moving out of the waste rock and to the surface are calculated in

grams per day as the product of flow rate (liters per minute) and concentration (milligrams per liter). Plots of uranium and zinc are presented in figure 8. This figure again shows an increase in the mass of metal ions with increase in flow. It is also apparent that during several months of high flow, large quantities of toxic metals were brought to the surface in solution at this one location.

Possible Flow Path

Investigators have speculated that a flow path exists between pit 3 and Boyd Seep. The water elevation in pit 3 was approximately 4.6 m (15 ft) higher than the elevation of Boyd Seep (fig. 4), and a fracture set is oriented along a line between pit 3 and Boyd Seep. Pit 3 is filling with water pumped back from collector wells, local infiltration, and direct precipitation. As the water elevation rises in the pit, the hydraulic gradient increases toward Boyd Seep, suggesting that water might be moving through a fracture in the calc-silicate formation and emerging at Boyd Seep.

The computer programs WATEQ4F and BALANCE were used to assist in evaluating such a flow path. The saturation indices for pertinent mineral phases are given in table A-12.

The water at both pit 3 and Boyd Seep is undersaturated with respect to most of the major primary mineral phases. The water in pit 3 appears to be in equilibrium with secondary mineral phases, such as gibbsite and kaolinite. The saturation indices for Boyd Seep are of similar sign and magnitude, except for gypsum. Calcium concentrations are apparently controlled by gypsum saturation. Iron speciation from WATEQ4F gives the principal solution species as Fe^{3+} and FeSO_4^0 at both locations. The saturation indices show that the water is saturated for goethite and undersaturated for ferrihydrite.

The water at Boyd Seep has higher concentrations of most of the reaction products from acid water formation than does the water from pit 3 (table 3), which is consistent with water movement from pit 3 to Boyd Seep. The water from pit 3 may be moving through the waste rock and upper part of the calc-silicate formation, dissolving the more easily weathered minerals, and emerging in a more highly concentrated form at Boyd Seep. To test this hypothesis, BALANCE was run on these waters. The mineral phases used were based on the mineralogical analyses of drill cuttings from well 89-1,⁷ which lies between pit 3 and Boyd Seep. The best models (7A, 7B, 7C, and 7D) are shown in table A-15.

In each of the four models, gypsum is formed. This agrees with the saturation index for gypsum at Boyd Seep as calculated by WATEQ4F. Amorphous silica is also

formed in all cases; this is also consistent with the trend in saturation indices. Pyrite and oxygen are consumed at a ratio of 3.79, which is very close to the theoretical ratio of 3.75 for pyrite oxidation. Goethite is precipitated in all models and maintains the low Fe^{3+} concentrations along the flow path. Minerals containing zinc and nickel are consumed, which increases the concentrations of these metals in solution.

Differences in the carbon balance show up in the models. In one pair of models, the carbon originates in calcite, while in the other, the source is carbon dioxide. Calcite is abundant in the drill cuttings from well 89-1. The negative saturation indices and the abundance of calcite indicate that this is the best choice for the carbon source.

Another difference in the models is the minerals dissolved to supply the aluminum; in one pair of models, Camontmorillonite dissolves, and in the other, gibbsite dissolves. The saturation indices show that either mineral would dissolve along the flow path.

The concentration of manganese decreases along the flow path. The saturation indices for manganite and pyrolusite, which are the most probable mineral phases that would control manganese concentrations under equilibrium conditions [Lindsay, 1979 (6)], are both very large negative

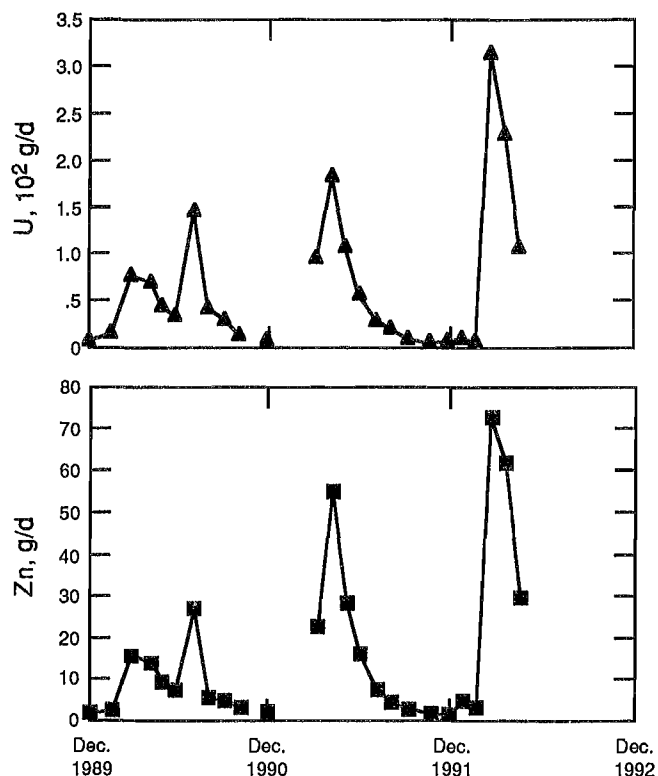


Figure 8.—Temporal variations in mass of released metals at Boyd Seep.

⁷Mineralogical analyses were performed by Charles N. Alpers under an interagency agreement between the USBM and USGS.

numbers. It is possible that an error in analysis occurred. However, the ICP-AES is very sensitive for the analysis of manganese and the difference was seen each time the samples were taken, so the measured values are probably correct.

On the other hand, there may be another mineral phase controlling concentrations that has not been included in the modeling. For example, phosphate concentrations may be high enough to precipitate a portion of the manganese. The ion chromatograph requires dilution of the sample prior to analysis because of the sulfate levels, so no quantitative data for phosphate were obtained. Spectrophotometric measurements will be attempted in the future.

Other possible sources of the water at Boyd Seep were investigated because field observations suggested that the seep originates, at least in part, from surface sediments connected to the seep by a short flow path. For example, the flow at Boyd Seep responds rapidly to precipitation events. Also, contaminated water was discharged at Boyd Seep even when the water level in pit 3 was below the level of the seep.

Therefore, waters from well 89-1 and Boyd Seep were compared. Well 89-1 is northwest of Boyd Seep with completions in the waste rock and just into the calc-silicate formation (fig. 5A). Assuming that some of the flow might originate in this formation, BALANCE was used to model the mixing of water from well 89-1S and well 89-1M to produce water of the type found at Boyd Seep.

The water from well 89-1S contains high concentrations of sodium (table 3). The source is probably albite, which has a negative saturation index (table A-12). If water flows from well 89-1S to Boyd Seep, dilution is necessary to lower the sodium to the level measured at the seep. The water from well 89-1M has lower concentrations of sodium and therefore was selected as the mixing water. Also, it seems reasonable that there would be some mixing of these two waters as they move downslope to Boyd Seep. The BALANCE information is given in tables A-16 to A-18.

Mineral phase dissolution is consistent with the saturation indices (table A-12). The dissolution of K-feldspar, diopside, and gibbsite produce the concentrations of calcium, magnesium, potassium, and aluminum measured in Boyd Seep water. As discussed previously, the precipitation of silica along the flow path is reasonable. Manganese levels are achieved by dissolution of pyrolusite, which is consistent with the saturation indices calculated for all three waters. As pH and Eh decrease, the solubility of manganese compounds increase [Lindsay, 1979 (6)]. The oxygen-to-pyrite consumption ratio is 3.69, which is reasonable. Gypsum is precipitated, which agrees with the saturation index.

The concentration of sodium in the Boyd Seep water is achieved using only dilution. This is necessary because no

common minerals exist that precipitate sodium from solution, except at concentrations far greater than those measured at Boyd Seep. No significant amount of adsorption on cation exchange sites is reasonable because concentrations of calcium and magnesium increase significantly, and these ions will displace monovalent ions, such as sodium, from adsorption sites [Babcock, 1963 (1)].

However, model 8A does have a flaw. The mixing ratio of 24 pct well 89-1S water to 76 pct well 89-1M water is not consistent with changes in flow observed shortly after a precipitation event. It is unlikely that water flow in a formation and at a depth as that sampled in well 89-1M would respond so quickly. Most times, the flow would be more constant than what was observed.

The possibility that water with properties similar to the water sampled at well 89-6 might be infiltrating and mixing upslope from Boyd Seep was also investigated. This scenario would provide water that has moved downslope and water that has a short flow path, so that part of the water flow would be continual and part would be responsive to short-term precipitation events.

Using the water quality data from wells 89-6 and 89-1S (tables A-19 to A-21), 286 models were tested. Of these, two plausible models were found to satisfy the mass balance constraints (table A-21).

The first model presented (9A) shows that no mixing of well 89-1S water is necessary. This is a possible solution of mass balance constraints, since modeling Blood Pool water has shown that the waste rock can produce acid water using input water similar to water from well 89-6. The models given in table A-21 and models 5A and 5B (table A-11) are similar. Blood Pool is dry during winter and summer, but Boyd Seep flows all year, except during the winter when it freezes. This indicates that a longer flow path recharges Boyd Seep.

The second model (9B) gives a mixing ratio of approximately 27 pct well 89-1S-type water to 73 pct well 89-6-type water. This mixing provides a large component of infiltration water that would respond to precipitation events rapidly and a smaller component that would provide continual flow. The saturation index of gibbsite is consistent with the dissolution shown in the model. Pyrite oxidation, with a molar ratio of oxygen to pyrite of 3.67, occurs, lowering the pH (table 3), and iron concentrations are controlled by secondary mineral formation. Gypsum is formed, which is consistent with the differences in saturation indices for the three waters. Even though calcite was included in the input parameters, it does not appear in the models. The mass balance solution requires only loss of carbon dioxide to balance the difference in alkalinity seen in the input. Hydrogen ions are not included in BALANCE, so pH control is observed only indirectly.

Because other minerals are known to be in the waste rock, different minerals were investigated (tables A-22 to

A-24). Anorthite and dolomite were substituted for diopside and calcite. The change to dolomite from calcite forced the dissolution of more carbonate in the models, since dolomite is the only source of magnesium. This is probably a more reasonable control on pH than that seen in previous models. The mixing ratios are identical to those seen in previous models, which supports accepting the flow path from well 89-1S to Boyd Seep with mixing of infiltration water of a type similar to that found at well 89-6.

In summary, even though the water level in pit 3 was higher in elevation than that at Boyd Seep, no model was found consistent with the hydrologic response of the system that could produce the water with concentrations found at the Boyd Seep when the model included water from pit 3. The preferred model combines two types of waters that originate upslope from the seep. A portion of the flow originates in deeper waste rock that produces water throughout the year. Infiltration of rainwater into surface wastes provides a larger component that responds rapidly to precipitation events. Mixing water with concentrations similar to those found at wells 89-1S and 89-6, combined with dissolution of minerals found in the waste rock, produces water with the concentrations measured at Boyd Seep.

DRAINAGE FROM PROTORE PILE

The previous discussion of the seeps on the east side of the minesite indicates that oxidation of sediments containing waste rock from mining operations produces acid water and elevated concentrations of toxic metals. When mining operations ceased, several protore piles were left on the surface.

Drainage from one of the small piles collects in a depression on a roadway; the water was sampled when sufficient amounts were present (fig. 1, Sis Pool). This water has the lowest pH and the highest sulfate concentration of any sampling location at the mine, indicating extensive acid water production. However, water just above the pile is uncontaminated, and thus the water becomes very contaminated as it moves through the pile. To develop an idea of the amount of material that must be consumed before contaminant concentrations could reach those found in the pool, the computer programs were employed.

The water from the bottom of the protore pile has a short residence time in the pile, as indicated by the seasonal nature of the flow. Concentrations of dissolved species are controlled by the kinetics of dissolution of the solid phases, by the equilibrium conditions that develop in the protore pile, and by the solubility of species in the puddle. The WATEQ4F calculations show that the water is undersaturated for all the major primary minerals found at the mine (table A-25).

The pile has large pore spaces that allow oxygen to diffuse into the interior and form acid water. Infiltrating water washes the reaction products away from the pyrite surface, allowing the acid to then react with the other minerals [Nordstrom and Potter, 1977 (15)].

According to saturation indices calculated by WATEQ4F (table A-25), aluminosilicates are undersaturated and tend to dissolve, producing high concentrations of aluminum and silica. As the water moves through the pile, large amounts of secondary minerals may form. The sulfate concentration becomes high enough so that extensive ion pairing with aluminum occurs; aluminum solubility is apparently controlled by jurbanite. The high sulfate concentrations also cause gypsum to precipitate, regulating the concentration of calcium. Epsomite is still undersaturated, allowing the water to develop very high magnesium concentrations. Amorphous silica also forms, controlling the solution concentration. At the measured Eh and pH, the iron in solution is predominantly Fe^{2+} and FeSO_4^0 species, but concentrations are not high enough to precipitate melanterite. The solution is apparently undersaturated for ferrihydrite and saturated for goethite. Oxidation of the Fe^{2+} may be occurring slowly, allowing the more crystalline solid phase to form and control solution concentration [Schwertmann and Taylor, 1977 (19)]. Other minerals that contain toxic metals are dissolved, producing high concentrations of zinc, manganese, nickel, and uranium.

To obtain information on the quantity of mineral phases that would need to be consumed to achieve the concentrations found in the water emerging from the protore pile, BALANCE was run to compare well 89-6-type water with water from the puddle (tables A-26 to A-28). The output shows that a kilogram of water with the characteristics of water from well 89-6 would consume approximately 0.10 mol of pyrite to produce the sulfate concentrations found in a kilogram of water from the puddle. The model shows that silica would be precipitated and gibbsite would be dissolved, both findings that agree with WATEQ4F. When the input to BALANCE was changed to include other aluminum-containing mineral phases, gibbsite does not appear in the models, indicating that a wide variety of minerals from the site could be dissolved by the acid water to produce the type of water found in the puddle. These findings are consistent with field observations. Pieces of protore are disintegrating at the edges, and secondary minerals are forming in their place.

When the water draining from the protore pile is compared with surface water from other areas on the site, it is apparent that the protore piles are major contributors of toxic metals to the hydrologic system. As long as atmospheric oxygen is allowed to come into contact with the protore and the reaction products are allowed to be flushed by infiltration water, water quality on the site will continue to deteriorate.

PIT 3

As described earlier, pit 3 is the largest open pit on the mine property. The water level has been getting higher because of precipitation, overland flow, ground water flow, and pumpback of water from the pollution control pond, which includes water from the pumped seeps (fig. 1). BLM has collected data on the quantity of water pumped back to pit 3 and the total volume of water accumulated in pit 3 from 1985 through 1991. On the basis of calculations from these data, the pumpback system contributes about 60 ± 10 pct of the increase in the volume of water in pit 3. To evaluate the relative contributions of pumpback water and infiltration water, BALANCE was used to evaluate the mixing of well 89-6-type water with water from the pollution control pond. Input and output files are shown in tables A-29 to A-31.

The model was used to calculate a mixing ratio of approximately 54 pct pollution control pond water to 46 pct infiltration water, which is close to the ratio calculated from pumping records. The minerals incorporated in the model were similar to those used to produce acid water using water from well 89-6.

The concentration values in water from the pollution control pond input to BALANCE were higher than those from pit 3, indicating that infiltration water to pit 3 must be diluting the water pumped back from the pollution control pond. However, the output from the program shows that some minerals must also be dissolved by infiltration water to achieve the concentrations measured in pit 3. It is apparent that any reclamation activities will have to deal with water infiltrating pit 3. As this model shows, the water may contain products of acid water formation. As pit 3 is dewatered, the infiltration water will need to be monitored to determine if treatment is required before it is discharged.

PIT 3 SEEP

Pit 4 lies in the northern third of the minesite. Mining operations ceased in pit 4 before they were halted in pit 3, so water that accumulated in pit 3 was pumped into pit 4. Although no water has been pumped into pit 4 since 1982, the water elevations continued to rise in pit 4 until approximately 1988. Since that time, the water elevation in pit 4 has remained relatively constant except for minor seasonal fluctuations. The stability of the water elevation suggests that the pit is in dynamic equilibrium with the local ground water flow system. That is, the amount of water recharging the pit is equal to the amount of water evaporating and being discharged as ground water.

The flow path of the ground water discharging from pit 4 is not well understood, but at least two discharge paths are plausible. Either the ground water discharges through

the ancestral West Drainage or through the central part of the minesite toward pit 3. The flow may be split between the two flow paths.

Seeps are seen in the north headwall of pit 3, and it is proposed that these seeps originate at least in part from leakage out of pit 4. To evaluate this possible flow path, WATEQ4F was run using water quality data from pit 4 and the seeps at pit 3 (pit 3S) to evaluate the solubility controls on solution concentrations.

The WATEQ4F data for pit 4 and the pit 3 seeps show that many of the common minerals are undersaturated (table A-32). In particular, calcium concentrations appear to be in equilibrium with calcite or possibly dolomite, but not gypsum. Iron concentrations are very low, and Fe^{3+} species predominate in the solution. Iron concentrations appear to be supersaturated with respect to ferrihydrate. Manganese concentrations are in apparent equilibrium with the solid phases pyrolusite and manganite.

Judging from the appearance of the seeps when sampling, part of the discharge originates where the alluvium and the waste rock contact bedrock and part is probably fed via fractures in the metasedimentary rock. A model was developed in which water flowing from pit 4 (water with concentrations equivalent to water typically sampled in pit 4) (table 3) was mixed with water infiltrating through the surface materials (as represented by well 89-6) to produce water with the characteristics of the pit 3 seep. Previously, a model had been developed that described a flow path from pit 4 to the pit 3 seeps with no mixing,⁸ but the mixing model better reflects field observations.

Using the input given in tables A-33 to A-35, four mass balance solutions were found, two of which are presented. The major difference is in the mixing ratios for the initial waters. When a larger proportion of infiltration water is used (table A-35, model 15A), more minerals are dissolved. More goethite and silica are formed, which matches the concentrations measured in pit 3 seep water. Gypsum was not used in the model, since gypsum was shown to be unsaturated in all three waters. Well 89-6 water is unsaturated for manganese, which would account for the dissolution of pyrolusite seen in the model. The oxygen-to-pyrite ratio is about 3.65, which is near the theoretical value.

In an attempt to decide which of the two models might best describe the proposed flow path, other models were developed using the same aqueous input but different mineral phases. Anorthite was substituted for diopside, which provides a different silica-to-calcium ratio. As a source of magnesium, dolomite was substituted for calcite.

Two models were produced that satisfied the mass balance constraints; one of these models (15C) is given in table A-35. The models differ only in whether or not the

⁸See footnote 7.

silica and aluminum concentrations are controlled by silica and kaolinite or by silica and gibbsite; the mixing ratios are the same. The saturation indices indicate apparent control by silica and gibbsite (table A-32). The mixing ratios agree closely with model 15B, indicating that the ratios of waters mixing to form the seeps may be about 89 pct pit 4 water to 11 pct infiltration water.

From the field observations and models, it is reasonable to believe that a hydrologic connection exists between pit 3 seep and pit 4, and that part of the water in pit 4 discharges to the seeps in the headwall of pit 3. However, the amount of this discharge is small, from 3.4 to 7.2 L/min (0.9 to 1.9 gal/min). Thus, discharge from pit 4 is probably draining to other areas that should be studied in subsequent phases of the site investigation.

WELL 89-3

Well 89-3 provided a sampling location at which to investigate a hydrologic connection between the aquifer in the breccia and the upper part of the metasediments, and the aquifer in the quartz monzonite intrusive. The water sampled in well 89-3 is moving according to the gradient shown by the contours in figure 6. The concentrations of ions in solution are being produced by chemical reactions in the rock formation upgradient from the well. Even though the sampling zone at well 89-3D is approximately 15 m (50 ft) below the sampling zone at well 89-3M (fig. 5C), the water level in the 89-3D zone stays 0.3 m (1 ft) higher than in 89-3M zone (fig. 9). This difference indicates that a region of low permeability lies between the zones. Also, it is unlikely that water is moving from well 89-3M to well 89-3D. This means that the aquifer in the metasediments is independent of the aquifer in the quartz monzonite intrusive, at least at this location.

Well 89-3M is another location where the characteristics of acid mine water are illustrated (table 3). The water has reacted with carbonate minerals in a slightly reducing environment so that the acid has been neutralized by the carbonates. The pH and the alkalinity are significantly higher than at Blood Pool, and the Eh is somewhat lower. The pH has risen high enough so that the Fe^{3+} is only slightly soluble. However, the Eh is low enough that the principal iron species are Fe^{2+} and $\text{FeSO}_4^0(\text{aq})$, and the solubility is much higher. The lower Eh correlates with a lower DO value than at Boyd Seep. Indeed, when a sample of this water was exposed to atmospheric oxygen, the water became turbid with what appeared to be a red-brown precipitate of ferrihydrite, indicating that the Fe^{2+} had oxidized and precipitated.

Water from well 89-3D has a much lower specific conductance than water from well 89-3M (table 3). The higher pH, higher Eh, and higher DO indicate a zone where less acidic water had been produced. The alkalinity is

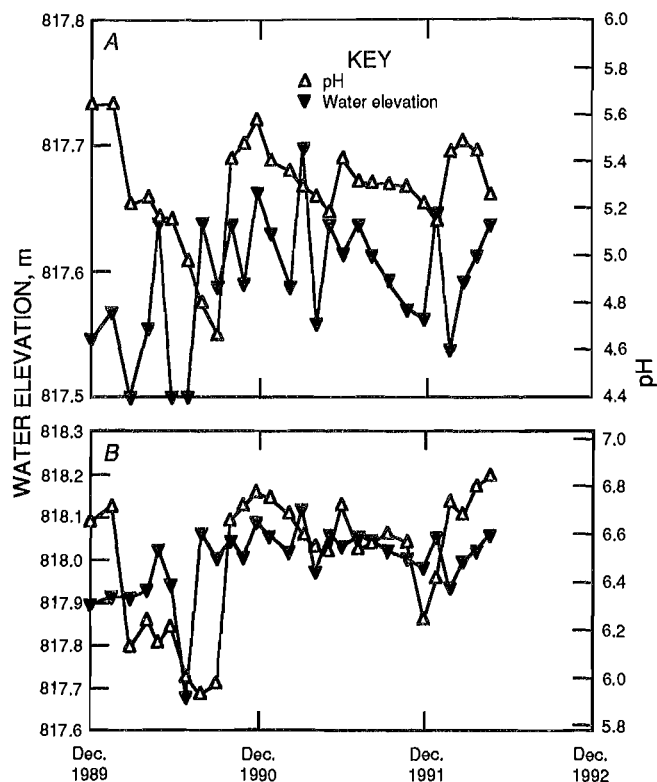


Figure 9.—Temporal variations in water level and pH. A, Well 89-3M; B, well 89-3D.

close to that of well 89-5D, discussed as an example of an uncontaminated zone. The sulfate levels indicate that acid water has been produced but neutralized, as shown by the concentrations of calcium and magnesium. At the higher Eh and pH levels, Fe^{3+} , which has a much lower solubility, predominates.

To obtain information on the relative changes in water quality that have occurred on the site during the study period, ion concentration data from well 89-3 were plotted as a function of time (figs. 10-11).

Figure 10 shows a continual increase in dissolved constituents in water from well 89-3M. Iron and sulfate, which are reaction products from pyrite oxidation, and toxic metal concentrations, represented by uranium and zinc, increase steadily. The products from neutralization of the acidic water (pH 3.5), as indicated by the concentration of magnesium, also increase. Calcium concentrations are roughly constant because of the solubility control by gypsum, which is consistent with the saturation index calculated by WATEQ4F (table A-36). The pH is the only parameter measured that appears to fluctuate seasonally (fig. 9A). The reason for the pH fluctuations while metal concentrations rise steadily has not been determined.

The concentrations of the same ions (sulfate, calcium, and magnesium) shown to be increasing in well 89-3M decrease in the water in well 89-3D (fig. 11), but these

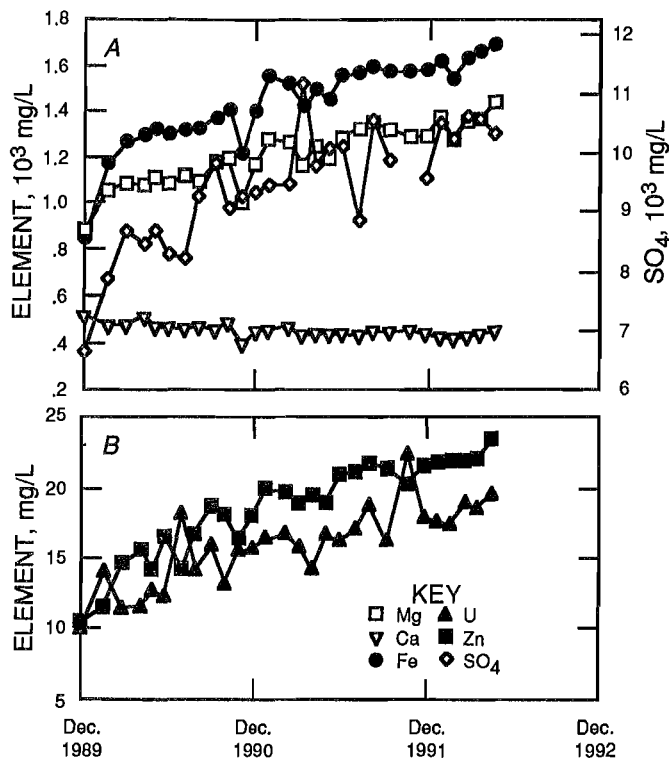


Figure 10.—Temporal variations in ground water quality at well 89-3M. A, Calcium, magnesium, iron, and sulfate; B, uranium, zinc, and pH.

concentrations appear to be leveling off. Gypsum is not controlling calcium levels. Iron and uranium concentrations drop below detection limits (0.008 and 1 mg/L, respectively). With the information available at this time, no conclusion can be reached concerning the reasons for the decrease.

The higher water level in well 89-3D, compared with that in well 89-3M, indicates that no water is moving from the metasediments to the quartz monzonite intrusive. The high concentration of ions in the water from well 89-3M shows that the water originates in an area producing large amounts of acidic water, implying that there is a connection between the water in the metasediments and in the protore pile above it. The probable flow path is lateral within the metasediments at the contact with the intrusive.

WELL 89-4

Temporal Changes

Well 89-4 was completed next to a protore pile, allowing water in two zones to be sampled (figs. 1 and 5D). This protore pile has been identified as containing some of the most reactive material on the minesite. Temporal variations in water elevation and water quality indicated

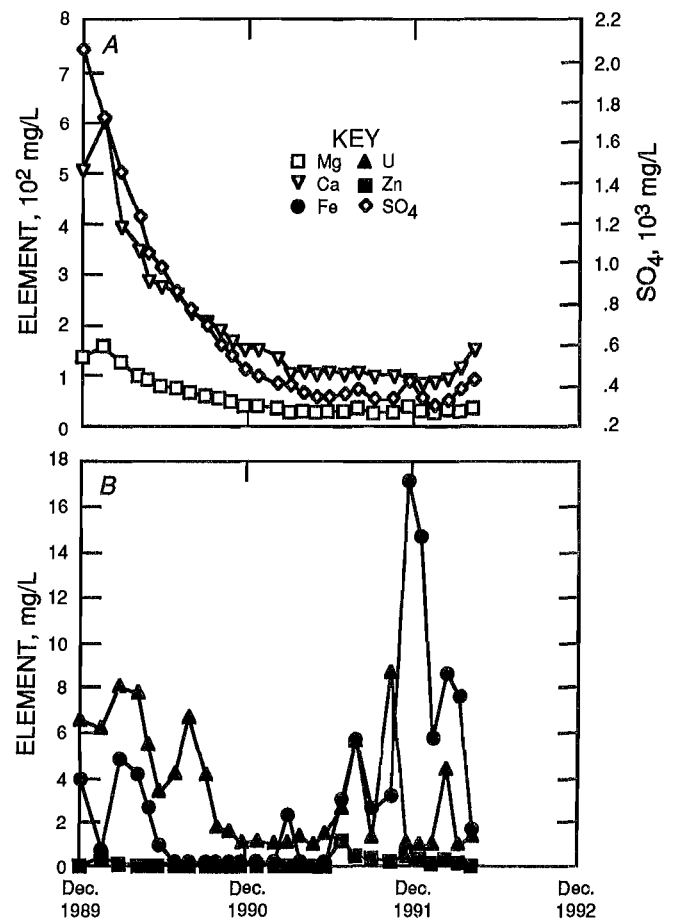


Figure 11.—Temporal variations in ground water quality at well 89-3D. A, Calcium, magnesium, and sulfate; B, uranium, zinc, and iron.

that chemical reaction products were being flushed from sites in the waste rock and moved downgradient.

Water elevation varied by approximately 0.3 m (1 ft) throughout the year, reaching a minimum in the winter and maximums during the spring and summer. In addition, while water quality was poor to begin with, pH decreased from 5.5 at the beginning of the study to almost 4 during the winter and spring of 1991. At the same time, concentrations of many ions increased (fig. 12).

For example, sulfate and magnesium concentrations showed two types of temporal variation. First, they varied annually in response to changes in water elevation, indicating infiltration by snowmelt and rain. Second, they increased steadily over the duration of the study. These two types of variation indicate that well 89-4S is being impacted by reaction products from the protore pile. The steady increase in concentrations of uranium, zinc, and iron also support this hypothesis.

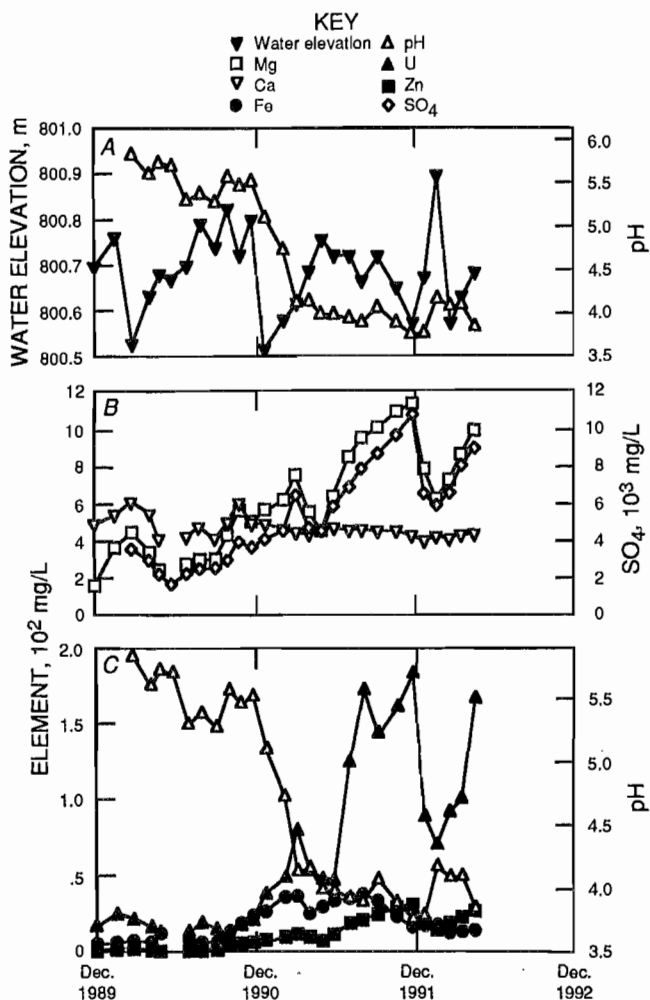


Figure 12.—Temporal variations in water level and ground water quality at well 89-4S. A, Water level and pH; B, calcium, magnesium, and sulfate; C, uranium, zinc, iron, and pH.

Calcium concentrations are controlled by gypsum saturation as shown by the saturation index calculated by WATEQ4F (table A-37). Seasonal variations stopped after December 1990; at that time, sulfate concentrations had increased to the point where gypsum saturation and subsequent precipitation occurred. Since that time, there have been only minor variations in calcium levels.

Proposed Flow Path From Well 89-4S to South Spoils Seep

The water in well 89-4S comes from the waste rock at the surface and is similar to that coming out of the protore pile at the Sis Pool site, which indicates that well 89-4S is another example where acidic water is produced after being partly neutralized by carbonate-containing minerals (table 3). The differences in water chemistry between the two zones at well 89-4 are similar to the differences described for the two zones at well 89-3.

The sampling location called the South Spoils Seep is a drain pipe that collects water from the South Spoils. The drain outflow lies below the high-water mark of the pollution control pond, and a sample was taken whenever the drain was above water level. As is apparent from the analytical results (table 3), the water is very contaminated.

Sources of water to the South Spoils Seep may be from the area of well 89-4S or from waste rock or from a combination of both. A model in which water from these two sources is mixed was generated to evaluate the relative contributions from each source and to determine if a flow path from well 89-4S to South Spoils Seep was plausible. The saturation indices are shown in table A-37, and the input and output files for BALANCE are given in tables A-38 to A-40.

To achieve ground water of the quality found at the South Spoils Seep, approximately 58 pct of the flow could be coming from water with the chemical characteristics of water found in well 89-4S and 42 pct could be coming from infiltration water. The model shows that large amounts of pyrite are consumed in the highly oxygenated South Spoils. This would be consistent with the high DO (10 mg/L) measured at the South Spoils Seep and the low pH. Because pyrite is considered a waste material, it also seems logical that a major portion of the pyrite would have been discarded in the South Spoils. During mining, particle sizes of the waste rock were reduced, which increased the surface area. The South Spoils is an optimum environment for acid water production.

Fe³⁺ is only slightly soluble in highly oxygenated water at pH >3.5. Both measured values and the model reflect this situation where concentrations of iron are controlled by secondary minerals (goethite). Large amounts of gibbsite and kaolinite should be dissolved, according to the model. The WATEQ4F results show that both gibbsite and allophane are undersaturated. Kaolinite has a positive saturation index at well 89-4S, but a negative one at the South Spoils Seep. This means that large amounts of aluminum could be entering solution from crystalline or amorphous materials. The aluminum values (table 3) show roughly twice the concentration at South Spoils Seep as at well 89-4S. This finding is consistent with measured pH, since aluminum solubility increases as pH decreases.

The model shows a large quantity of silica being precipitated in the flow path, which agrees with the differences seen in the saturation indices for silica. Calcium concentrations decrease between well 89-4S and South Spoils Seep. The increase in sulfate concentrations caused by acid water production decreases the concentration of calcium because gypsum is being precipitated. The model and the analytical data show that minerals containing toxic metals, such as uranium, zinc, or manganese, will be dissolved and concentrations will increase along the flow path because of the low pH.

The flow path model and equilibrium chemical reactions show that low-quality water from the areas around the protore piles and degradation of infiltration water within the South Spoils may contribute to the contaminated water emerging at South Spoils Seep. The protore piles are being oxidized and produce high concentrations of dissolved solids. Good-quality infiltration water reacts with minerals expected to be found in the waste rock to produce conditions of low pH and large amounts of dissolved solids. Both areas may contribute to acid water formation and the elevated levels of toxic metals measured in the water at the South Spoils Seep.

EAST DRAINAGE SURFACE RUNOFF

Transport of the products of chemical reactions to areas off the minesite is one of the major concerns of the current research. The East Drainage Control sampling location is upgradient from major sources of contamination, assuming a north-south primary ground water flow path. Water movement from the area around the water treatment plant and the Blood Pool may contribute to the slightly elevated sulfate concentrations measured at East Drainage Control. The quantity of contamination entering the drainage upstream is minor. As noted in the section "Ground Water Elevations and Flow Paths," the higher water elevation measured at well 89-5 indicates that the ridge blocks eastward contaminant migration.

Water quality deteriorates between East Drainage Control and East Drainage 11. The specific conductance approximately doubles (table 3) while the alkalinity remains roughly constant. Sulfate levels increase by about a factor of 10, while calcium and magnesium concentrations doubled. (Elevated sulfate concentrations in conjunction with elevated calcium and magnesium concentrations indicate acid water that has been neutralized by carbonate-bearing minerals.)

Temporal variations in water quality—that is, increases in sulfate concentrations during spring runoff—at East Drainage Control indicate that minor flushing of reaction products from acid water formation occurs in the spring (fig. 13A). Calcium and magnesium concentrations remain more or less constant. It is possible that contaminated water is coming from the area near Boyd Seep.

Downstream at East Drainage 11 the opposite trend is seen (fig. 13B). Sulfate concentrations decrease during spring runoff and increase during the summer at low flow. This sequence could indicate a continuously flowing source of water with high sulfate concentrations that is diluted by runoff in the spring.

The WATEQ4F saturation indices show the equilibrium control on the water at East Drainage Control and East Drainage 11 (table A-41). Water from these locations is slightly below saturation with respect to amorphous silica, saturated with respect to gibbsite, and unsaturated for

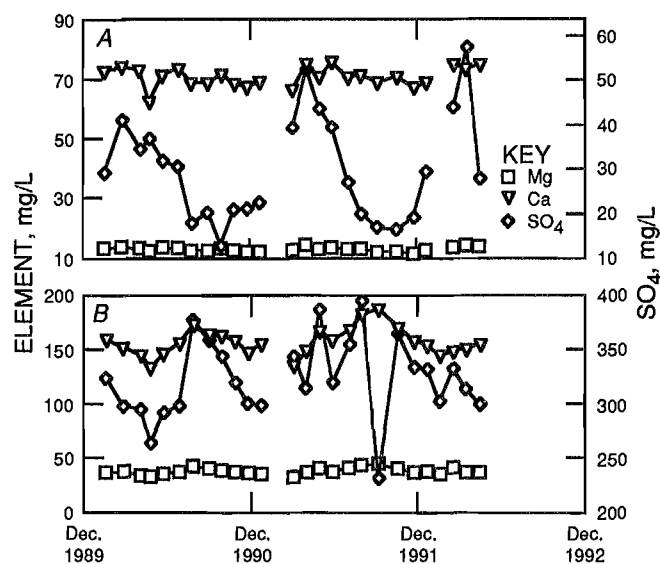


Figure 13.—Temporal variations in calcium, magnesium, and sulfate. A, East Drainage Control; B, East Drainage 11.

gypsum. The principal iron species is Fe^{3+} ; the water is saturated with iron according to the value calculated for ferrihydrite. Carbonate is in equilibrium with dolomite, which controls the concentration of calcium and magnesium at this pH.

To obtain information on the relative contributions that a source of acid water would have on water at East Drainage Control, BALANCE was run where Boyd Seep water was mixed with East Drainage Control water to produce East Drainage 11 water (tables A-42 to A-44). To compensate for different rates of flow, concentration was multiplied by flow rate. The values used for the model came from samples collected in April 1991. The flow rates were 38 L/min (10 gal/min) at East Drainage Control, 76 L/min (20 gal/min) at East Drainage 11, and 2 L/min (0.55 gal/min) at Boyd Seep. The mixing ratios showed that about 10 pct of the material at East Drainage 11 could come from a source with concentrations similar to those found at Boyd Seep.

To achieve the concentrations of calcium, magnesium, and sulfate at East Drainage 11, significant quantities of the acid water products must be added to the system. These products may come from other point sources yet undiscovered or from nonpoint sources in the alluvium. BALANCE shows that oxygen and pyrite are consumed to produce the sulfate levels shown in table A-43 with an oxygen to pyrite ratio of 3.75. The pH is maintained above 7 by reactions with carbonate-bearing minerals such as dolomite. The secondary minerals gibbsite, silica, and goethite are also formed, which agrees with the WATEQ4F data.

Both the measured flow rates and the computer-modeled analytical data indicate that point and nonpoint

sources of contamination degrade the water leaving the site on the eastern side of the mine. Highly contaminated water moves through the central portion of the site. The western side of the mine has fewer sampling locations, yet the water collected from seeps at West Drainage and West Drainage Control indicates that large quantities of poor-quality water are also being produced on this side (fig. 1).

WEST DRAINAGE

Only one well (89-7) was installed in the West Drainage; this well had one completion zone from which water samples from the intrusive were taken (fig. 1). The elevation of the completion is approximately the same as for well 89-3D, and the water quality was similar to water from well 89-3D (table 3); that is, there are low concentrations of the products of acid water formation. The Eh and pH are relatively high, which limits the solubility of the types of toxic metals studied in this project. The similarities in the water indicate that the contaminants seen in the waste rock and protore piles have not infiltrated the intrusive to any significant extent.

Downslope from well 89-7, at the toe of the South Spoils, two seeps (the West Drainage Seep and the West Drainage Control Seep) emerge near an area close to a point where a stream existed before mining began (figs. 1-3). Water quality is very similar at both seeps—acidic and partially neutralized by reactions with carbonate minerals—and is also similar to water from Boyd Seep. These seeps are major sources for the water pumped into the pollution control pond and then into pit 3.

Characteristics of drainage in the area have changed since the beginning of mining. The stream was once seasonal, drying up during the summer months, but now the pumps at the West Drainage operate year round. This indicates that the mine waste has increased the quantity of water being retained on the slope; the waste rock stores water instead of allowing it to leave the area as overland flow during spring runoff. The water emerges at the seeps after moving through the waste rock, which provides the opportunity for the water to react with the wastes. To obtain information on speciation and solubility controls in the water from well 89-7 and West Drainage Control, WATEQ4F was run using data from these locations.

The saturation indices also show that water from well 89-7 (table A-45) and well 89-3D (table A-36) and from West Drainage Control (table A-45) and Boyd Seep (table A-12) are very similar. Again, it was concluded that there is very little migration of contaminants from the waste rock into the intrusive, which indicates that the affected zone on the west side of the mine has not extended vertically to any significant extent. At the present time, however, the project has no sampling site on the west side to use in modeling flow paths.

Judging from the large volume and the low quality of the water being pumped from the seeps at West Drainage and West Drainage Control, it is obvious that acid water formation is occurring on the west side of the mine. The next phase of the project will be to evaluate where sampling wells should be installed to help elucidate flow paths in this area.

CONCLUSIONS

Geochemical modeling has advanced the understanding of the hydrogeology of the Midnite Mine by delineating possible flow paths on the basis of hydrochemical changes in water quality between sampling sites. Even though the system as defined by thermodynamics is continually changing, computer models based on thermodynamic equilibria are useful in describing solubility control of solution species.

Acid water is being produced in protore piles, waste rock, and other spoils piles because of the oxidation of sulfide-containing minerals, such as pyrite, associated with the ore and waste materials. The acid water dissolves minerals in the piles, which may raise pH or may increase concentrations of toxic metals in the water.

Seasonal flushing of contaminated water occurs at several locations at the Midnite Mine. Water containing high concentrations of toxic metals is produced when rainwater moves through the protore piles and migrates

downgradient away from the piles, and at several seeps, concentrations of toxic metals increase as the flow rate increases. This indicates that soluble products built up in the protore piles during the dry season are being dissolved by infiltration water.

The volume of water in pit 3 is continually increasing as a result of precipitation, ground water flow, overland flow, and pumpback of water from the pollution control pond. On the basis of geochemical modeling of concentrations of major cations and anions from various sources, the water entering pit 3 from infiltration and runoff is being degraded and may require treatment before it is discharged from the site.

Ground water emerging at Boyd Seep is probably a mixture of water from the area near well 89-1 and water infiltrating the waste rock just above the seep. A mixture of water from these sources would explain the seasonal fluctuations in flow and metal concentrations measured at

the seep, as well as account for the continual flow at the seep during the summer months. Although a flow path may exist between pit 3 and Boyd Seep, the hydrochemical models indicate that such a flow path is unlikely.

A hydraulic connection between pit 4 and the seeps on the north headwall of pit 3 is probable. The hydrochemical models describe the water from the seeps as predominantly pit 4 water with a smaller component of infiltration water. The quantity of water being discharged, however, is very small.

The higher water level measured in the deep completion of well 89-3 in the intrusive as compared with water levels in the middle completion indicates that no water is moving into the intrusive at this location. The higher concentrations of toxic metals in the water from the middle completion show that the water originates in an area producing large amounts of acid water, implying that a connection exists between the water in the metasediments

and the protore pile above it. The probable flow path is lateral within the metasediments at the contact with the intrusive.

A flow path model showed that contaminated water from the areas around the protore piles, as sampled at well 89-4S, and degradation of infiltration water within the South Spoils may contribute to the contaminated water emerging at the South Spoils Seep. Both areas may be responsible for the elevated concentrations of heavy metals and the low pH measured at the South Spoils Seep.

Concentrations of those ions that indicate acid water production have increased significantly at several sampling locations since November 1989. Concentrations of toxic metal ions have also increased at those sites. This finding indicates that deterioration of water quality at the Midnite Mine can be expected to continue until the causes of acid water production are controlled.

RECOMMENDATIONS FOR FUTURE RESEARCH

A picture of the geochemistry of the Midnite Mine is beginning to emerge after the evaluation of 28 months of data. However, several geochemical topics need further investigation, and the information on the geochemistry at the site should be merged with information on the hydrology. This information is required to provide the baseline data necessary for mine reclamation.

Sample collection frequency should be modified. A monthly sampling schedule is not the most cost-efficient scheme to provide the information necessary for site hydrochemical evaluation. The scheduling of sample collection based on climatic events would provide a better assessment of changes that occur seasonally, especially during spring runoff. Sample collection during winter and summer could be done less often than once a month but more often during hydrologic changes in the spring.

Geophysical tests need to be used to assist in understanding more of the original geology, much of which is now obscured by waste rock. This information would provide a better assessment of potential flow paths. Geophysical studies could also be used to place additional sampling wells at optimal locations.

Additional ground water sampling wells need to be installed in the West Drainage. These wells should be placed to help determine the origin of the contaminated water that emerges at the seeps to the west (West Drainage and West Drainage Control).

Better methods of analyzing for phosphate and chloride need to be developed. The phosphate values will assist in

determining possible means of controlling heavy metal concentrations in the ground water through precipitation of secondary phosphate minerals. The chloride values will assist in BALANCE models when developing mixing ratios. It is a conservative ion whose concentration is not controlled by precipitation at the Midnite Mine.

Control of heavy metal concentrations and slowing metal mobility by adsorption mechanisms need to be evaluated. Preliminary data from analyses of sediments from the bottom of pit 3 indicate that heavy metal adsorption on the surface of secondary minerals is occurring. Experiments should be started to investigate the reversibility of the adsorption reactions. This would provide information concerning problems that might occur as pit 3 is emptied and the sediments are exposed to fresh infiltration water.

Using the water level data from the existing wells, ground water flow modeling on the site should be completed. After wells are installed in the western section of the mine, a hydrologic contour map should be drawn for each of the hydrologic zones. Particular attention needs to be focused on the apparent anomaly at well 89-3.

A water budget for pit 4 needs to be developed. This would assist in answering questions as to whether the pit will remain dry after it is emptied and whether use of the pit can be used as a repository for reactive rock.

After the hydrologic contour map is developed, it should be merged with the computer modeling information in this RI to generate a description of possible flow paths at the mine.

REFERENCES

1. Babcock, K. L. Chemical Properties of Soil Colloids. *Hilgardia*, v. 34, No. 11, 1963, pp. 417-542.
2. Ball, J. W., and D. K. Nordstrom. User's Manual for WATEQ4F, With Revised Thermodynamic Data Base and Test Cases for Calculating Speciation of Major, Trace, and Redox Elements in Natural Waters. U.S. Geol. Surv. OFR 91-183, 1991, 193 pp.
3. Ball, J. W., D. K. Nordstrom, and D. W. Zachman. WATEQ4F—A Personal Computer Fortran Translation of the Geochemical Model WATEQ2 With Revised Data Base. U.S. Geol. Surv. OFR 78-50, 1987, 108 pp.
4. Fleschman, B. R., and S. P. Dodd. Ritzville Quadrangle, Washington. National Uranium Resource Evaluation Program. Bendix Field Eng. Corp., Grand Junction, CO, 1982, 62 pp.
5. Freeze, R. A., and J. A. Cherry. *Ground Water*. Prentice-Hall, 1979, 604 pp.
6. Lindsay, W. L. *Chemical Equilibria in Soils*. Wiley, 1979, 449 pp.
7. Lowson, R. T. Aqueous Oxidation of Pyrite by Molecular Oxygen. *Chem. Rev.*, v. 82, No. 5, Oct. 1982, pp. 461-497.
8. Ludwig, K. R., J. T. Nash, and C. W. Naeser. U-Pb Isotope Systematics and Age of Uranium Mineralization, Midnite Mine, Washington. *Econ. Geol.*, v. 76, No. 1, 1981, pp. 89-110.
9. Milne, P. C. Uranium in Washington State: Proven Deposits and Exploration Targets. *CIM Bull.*, v. 72, No. 804, 1979, pp. 95-101.
10. Nash, J. T. *Geology of the Midnite Uranium Mine Area, Washington: Maps, Description, and Interpretation*. U.S. Geol. Surv. OFR 77-592, 1977, 38 pp.
11. Nash, J. T., and N. J. Lehrman. *Geology of the Midnite Uranium Mine, Stevens County, Washington: A Preliminary Report*. U.S. Geol. Surv. OFR 75-402, 1975, 36 pp.
12. National Resource Ecology Laboratory. *Precipitation Chemistry. National Atmospheric Deposition Program/National Trends Network*. CO State Univ., Fort Collins, CO, Jan.-June 1987, 193 pp.
13. Nordstrom, D. K. Aqueous Pyrite Oxidation and Consequent Formation of Secondary Iron Minerals. Ch. in *Acid Sulfate Weathering*. *Soil Sci. Soc. Amer.*, 1982, pp. 37-56.
14. Nordstrom, D. K., E. A. Jenne, and J. W. Ball. Redox Equilibria of Iron in Acid Mine Waters. Ch. in *Chemical Modeling in Aqueous Systems: Speciation, Sorption, Solubility and Kinetics*, ed. by E. A. Jenne. *Amer. Chem. Soc. Symp. Ser.* 93, 1979, pp. 51-79.
15. Nordstrom, D. K., and R. W. Potter II. The Interactions Between Acid Mine Waters and Rhyolite. Paper in *Proceedings of Second International Symposium on Water-Rock Interactions*, Strasbourg, France, I, 1977, pp. 15-26; available from A. D. Marcy, Spokane Res. Cent., BuMines, Spokane, WA.
16. Parkhurst, D. L., L. N. Plummer, and D. C. Thorstenson. BALANCE—A Computer Program for Calculating Mass Transfer for Geochemical Reactions in Ground Water. U.S. Geol. Surv. Water-Resour. Invest. Rep. 82-14, 1982, 29 pp.
17. Plummer, L. N., E. C. Prestemon, and D. L. Parkhurst. An Interactive Code (NETPATH) for Modeling NET Geochemical Reactions Along a Flow PATH. U.S. Geol. Surv. Water-Resour. Invest. Rep. 91-4078, 1991, 227 pp.
18. Robbins, D. A. Applied Geology in the Discovery of the Spokane Mountain Uranium Deposit, Washington. *Econ. Geol.*, v. 73, 1978, pp. 1523-1538.
19. Schwertmann, U., and R. M. Taylor. Iron Oxides. Ch. in *Minerals in Soil Environments*. *Soil Sci. Soc. Amer.*, 1977, pp. 145-180.
20. Sposito, G. Soil Minerals. Ch. in *The Chemistry of Soils*. Oxford Univ. Press, 1989, pp. 22-39.
21. Steffan, Robertson, and Kirsten, Inc. (Lakewood, CO). Report on the Technology of Acid Generation and Metal Leaching From Solid Mine Waste. Rep. 63701/1, 1988, 130 pp.
22. Sumioka, S. S. Quality of Water in an Inactive Uranium Mine and Its Effects on the Quality of Water in Blue Creek, Stevens County, Washington, 1984-85. U.S. Geol. Surv. Water-Resour. Invest. Rep. 89-4110, 1991, 62 pp.
23. U.S. Environmental Protection Agency. *Methods for Chemical Analysis of Water and Wastes*. Publ. EPA-600-/4-79-020, 1983, 298 pp.
24. Washington State. *Water Well Construction Act of 1971, Minimum Standards for Construction and Maintenance of Wells*. WAC ch. 173-160, effective Mar. 13, 1990.
25. Wilding, L. P., N. E. Smeck, and L. R. Drees. Silica in Soils: Quartz, Cristobalite, Tridymite, and Opal. Ch. in *Minerals in Soil Environments*. *Soil Sci. Soc. Amer.*, 1977, pp. 471-557.

APPENDIX.—DATA USED IN GROUND WATER MODELING

Table A-1.—Saturation indices for selected minerals from WATEQ4F using analytical data from well 89-6 and well 89-5D

Mineral	Well 89-6	Well 89-5D
Albite	-1.904	0.503
Allophane (amorphous)680	1.203
Al(OH) ₃	-.141	-.052
Anorthite	-4.011	-.884
Calcite	-3.214	-.945
Ca-montmorillonite	6.462	7.569
Diopside	-12.440	-7.162
Ferrihydrite637	2.632
Gibbsite (crystalline)	2.677	2.773
Goethite	6.528	8.523
Gypsum	-3.471	-2.804
Jarosite K	-6.905	-2.690
Kaolinite	7.622	8.053
K-mica	9.882	13.041
Manganite	-6.476	-3.140
Pyrolusite	-10.561	-7.499
Quartz577	.872
Silica (amorphous)	-.609	-.494

Table A-2.—Input and output files from BALANCE comparing rainwater and water from well 89-6, millimoles per kilogram

Element	Final, well 89-6	Initial, rainwater
C	0.6671	0.0001
Ca1868	.0039
Fe0004298	.000
K002558	.0013
Mg1088	.0010
Na1790	.0076
RS	3.066	.035
S06621	.0059
Si3662	.000

RS Redox state of solution.

Table A-3.—Mineral and gas input data to BALANCE comparing rainwater and water from well 89-6

Constituent ¹	Element	Stochastic ratios in empirical formulas
Albite (+)	Na	1.0
	Al	1.0
	Si	3.0
Calcite (+)	Ca	1.0
	C	1.0
	RS	4.0
"CH ₂ O"	C	1.0
CO ₂ gas	C	1.0
	RS	4.0
Diopside (+)	Ca	1.0
	Mg	1.0
	Si	2.0
Goethite (-)	Fe	1.0
	RS	3.0
K-mica (+)	K	1.0
	Al	3.0
	Si	3.0
O ₂ gas (+)	RS	4.0
Pyrite (+)	Fe	1.0
	S	2.0
	RS	0.0
Silica (amorphous)	Si	1.0

RS Redox state of solution.

¹Plus = dissolving; minus = precipitating.

Table A-4.—Mineral and gas output data^{1,2} from BALANCE comparing rainwater and water from well 89-6

Constituent	Model 2A		Model 2B	
	Input con-straints ³	Output	Input con-straints ³	Output
Albite	+	0.1714	+	0.1714
Calcite	+	.0751	+	.0751
"CH ₂ O"5920		.5920
CO ₂ gas5920
Diopside	+	.1078	+	.1078
Goethite	-	-.0297	-	-.0297
K-mica	+	.0013	+	.0013
O ₂ gas	+	.7049	+	.1129
Pyrite	+	.0302	+	.0302
SiO ₂		-.3674		-.3674

¹Blank spaces indicate no figures are relevant.

²Millimoles of reactant or product per kilogram of final water.

³Plus = dissolving; minus = precipitating.

Table A-5.—Input and output files from BALANCE evaluating possible flow path from well 89-6 to well 89-5D, millimoles per kilogram

Element	Final, well 89-5D	Initial, well 89-6
Al	0.01112	0.01112
C	2.900	.6671
Ca	.7398	.1868
Fe	.003296	.0004298
K	.06722	.002558
Mg	.1638	.1088
Mn	.002809	.0001238
Na	1.317	.1790
RS	12.230	3.066
S	.1048	.06621
Si	.4695	.3662

RS Redox state of solution.

Table A-6.—Mineral and gas input data to BALANCE evaluating possible flow path from well 89-6 to well 89-5D

Constituent ¹	Element	Stochastic ratios in empirical formulas
Albite (+)	Na	1.0
	Al	1.0
	Si	3.0
Anorthite (+)	Ca	1.0
	Al	2.0
	Si	2.0
Calcite (+)	Ca	1.0
	C	1.0
	RS	4.0
	C	1.0
CO ₂ gas	RS	4.0
	C	1.0
	C	1.0
Diopside (+)	Ca	1.0
	Mg	1.0
	Si	2.0
Gibbsite (-)	Al	1.0
Goethite (-)	Fe	1.0
	RS	3.0
K-mica (+)	K	1.0
	Al	3.0
	Si	3.0
MnO ₂ (+)	Mn	1.0
	RS	4.0
O ₂ gas	RS	4.0
	Fe	1.0
Pyrite (+)	S	2.0
	RS	0.0
	Si	1.0

RS Redox state of solution.
¹Plus = dissolving; minus = precipitating.

Table A-7.—Mineral and gas output data¹ from BALANCE evaluating possible flow path from well 89-6 to well 89-5D

Constituent	Input constraints ²	Output
Albite	+	1.1380
Calcite	+	.4980
CO ₂ gas		1.7349
Diopside	+	.0550
Gibbsite	-	-1.3320
Goethite	-	-.0164
K-mica	+	.0647
MnO ₂	+	.0027
O ₂ gas		.0677
Pyrite	+	.0193
SiO ₂		-3.6147

¹Millimoles of reactant or product per kilogram of final water.

²Plus = dissolving; minus = precipitating.

Table A-8.—Saturation indices for selected minerals from WATEQ4F using analytical data from Blood Pool

Mineral	
Albite	-7.972
Allophane	-1.005
Anorthite	-16.509
Diopside	-18.683
Ferrihydrite	-1.724
Gibbsite (crystalline)	-2.328
Goethite	4.167
Gypsum	-.086
Jarosite K	.278
Jurbanite	.557
Kaolinite	-1.970
K-mica	-5.324
Pyrolusite	-11.528
Quartz	940
Silica (amorphous)	-.357

Table A-9.—Input and output files from BALANCE evaluating change of well 89-6-type water into Blood Pool water, millimoles per kilogram

Element	Final, Blood Pool	Initial, well 89-6
Al	3.324	0.01112
C	.000	.6671
Ca	11.050	.1868
Fe	.3039	.0004298
K	.1257	.002558
Mg	5.671	.1088
Mn	.5697	.0001238
Na	.9784	.1790
RS	155.00	3.066
S	25.800	.06621
Si	.7815	.3662
Zn	.01825	.000

RS Redox state of solution.

Table A-10.—Mineral and gas input data to BALANCE evaluating change of well 89-6-type water into Blood Pool water

Constituent ¹	Element	Stochastic ratios in empirical formulas
Albite (+)	Na	1.0
	Al	1.0
	Si	3.0
Anorthite (+)	Ca	1.0
	Al	2.0
	Si	2.0
Calcite (+)	Ca	1.0
	C	1.0
	RS	4.0
	C	1.0
CO ₂ gas (-)	RS	4.0
	Ca	1.0
Diopside (+)	Mg	1.0
	Si	2.0
	Fe	1.0
Goethite (-)	RS	3.0
	Ca	1.0
Gypsum (-)	S	1.0
	RS	6.0
	K	1.0
	Fe	3.0
Jarosite (-)	S	2.0
	RS	21.0
	Al	1.0
	RS	6.0
K-feldspar (+)	S	1.0
	K	1.0
	Al	1.0
Kaolinite (-)	Si	3.0
	Al	2.0
	Si	2.0
MnO ₂ (+)	Mn	1.0
	RS	4.0
O ₂ gas (+)	RS	4.0
	Fe	1.0
Pyrite (+)	S	2.0
	RS	0.0
	Si	1.0
	Zn	1.0
Sphalerite (+)	S	1.0
	RS	-2.0

RS Redox state of solution.

¹Plus = dissolving; minus = precipitating.

Table A-11.—Mineral and gas output data^{1,2} from BALANCE evaluating change of well 89-6-type water into Blood Pool water

Constituent	Model 5A		Model 5B	
	Input con-straints ³	Out-put	Input con-straints ³	Out-put
Albite	+	0.7994	+	0.7994
Anorthite	+	1.1952		
Calcite	+	4.1058	+	5.3010
CO ₂ gas	-	-4.7729	-	-5.9681
Diopside	+	5.5622	+	5.5622
Goethite	-	-12.5543	-	-7.7736
Jarosite			-	-2.3903
Jurbanite				
K-feldspar	+	.1231	+	2.5135
MnO ₂	+	.5696	+	.5695
O ₂ gas	+	47.5059	+	56.4696
Pyrite	+	12.8578	+	15.2481
SiO ₂	-	-15.8671	-	-20.6477
Sphalerite	+	.0183	+	.0183
	Model 5C		Model 5D	
	Input con-straints ³	Out-put	Input con-straints ³	Out-put
Albite	+	0.7994	+	0.7994
Anorthite			-	5.3010
Calcite	+	5.3010		
CO ₂ gas	-	-5.9681	-	-.6671
Diopside	+	5.5622	+	5.5622
Goethite				
Jarosite	-	-6.2771	-	-11.1068
Jurbanite	-	-5.1824	-	-19.3184
K-feldspar	+	7.6959	+	11.2299
MnO ₂	+	.5696	+	.5696
O ₂ gas	+	85.6207	+	125.3782
Pyrite	+	23.0217	+	33.62378
SiO ₂	-	-36.1950	-	-57.3990
Sphalerite	+	.0183	+	.0183

¹Blank spaces indicate no figures are relevant.

²Millimoles of reactant or product per kilogram of final water.

³Plus = dissolving; minus = precipitating.

Table A-12.—Saturation indices for selected minerals from WATEQ4F using analytical data from pit 3, Boyd Seep, well 89-1S, and well 89-1M

Mineral	Pit 3	Boyd Seep	Well 89-1S	Well 89-1M
Albite	-4.902	-4.855	-0.442	0.553
Allophane	-.764	-.714	.852	1.018
Al(OH) ₃	-2.584	-3.066	-1.543	-.312
Anorthite	-10.466	-11.562	-3.838	-.138
Calcite	-7.167	-6.300	-.774	-.198
Ca-montmorillonite	.323	-.051	3.184	7.658
Diopside	-15.481	-15.774	-6.530	-4.792
Ferrihydrite	-2.773	-3.839	2.034	2.452
Gibbsite (crystalline)	.194	-.237	1.247	2.491
Goethite	3.118	2.052	7.925	8.343
Gypsum	-.114	.023	-2.067	-1.475
Jarosite K	-6.421	-9.198	-2.692	-1.528
Kaolinite	2.587	2.129	4.492	7.804
K-mica	2.398	1.979	8.240	13.064
Manganite	-8.078	-8.363	-1.627	-2.651
Pyrolusite	-13.702	-14.912	-4.111	-5.690
Quartz	.707	.920	.610	1.024
Silica (amorphous)	-.625	-.447	-.730	-.325

Table A-13.—Input and output files from BALANCE evaluating flow path from pit 3 to Boyd Seep, millimoles per kilogram

Element	Final, Boyd Seep	Initial, pit 3
Al	2.904	1.857
C	.001646	.0001644
Ca	11.860	9.948
Fe	.004317	.02228
K	.3057	.1114
Mg	14.790	9.166
Mn	1.499	1.737
Na	2.836	2.341
Ni	.05561	.04734
RS	218.100	153.660
S	36.350	25.610
Si	.5083	.3774
Zn	.08145	.05725

RS Redox state of solution.

Table A-14.—Mineral and gas input data to BALANCE evaluating flow path from pit 3 to Boyd Seep

Constituent ¹	Element	Stochastic ratios in empirical formulas
Albite (+)	Na	1.0
	Al	1.0
	Si	3.0
Calcite (+)	Ca	1.0
	C	1.0
	RS	4.0
Ca-montmorillonite (+)	Ca	.167
	Al	2.33
	Si	3.67
CO ₂ gas (-)	C	1.0
	RS	4.0
Diopside (+)	Ca	1.0
	Mg	1.0
	Si	2.0
Gibbsite (+)	Al	1.0
Goethite (-)	Fe	1.0
	RS	3.0
Gypsum (-)	Ca	1.0
	S	1.0
	RS	6.0
K-feldspar (+)	K	1.0
	Al	1.0
	Si	3.0
MnO ₂ (+)	Mn	1.0
	RS	4.0
NiS (+)	Ni	1.0
	S	1.0
	RS	-2.0
O ₂ gas (+)	RS	4.0
Pyrite (+)	Fe	1.0
	S	1.0
	RS	0.0
SiO ₂	Si	1.0
Sphalerite (+)	Zn	1.0
	S	1.0
	RS	-2.0

RS Redox state of solution.

¹Plus = dissolving; minus = precipitating.

Table A-15.—Mineral and gas output data^{1,2} from BALANCE evaluating flow path from pit 3 to Boyd Seep

Constituent	Model 7A		Model 7B	
	Input con- straints ³	Out- put	Input con- straints ³	Out- put
Albite	+	0.4950	+	0.4950
Calcite	+	.0015	+	.0015
Ca-montmorillonite.			+	.1535
CO ₂ gas				
Diopside	+	5.6240	+	5.6240
Gibbsite		.3577		
Goethite	-	-7.2285	-	-7.2413
Gypsum	-	-3.7135	-	-3.7135
K-feldspar	+	.1943	+	.1943
MnO ₂	-	-.2380	-	-.2380
NiS	+	.0083		
O ₂ gas	+	27.3543	+	27.4024
Pyrite	+	7.2105	+	7.2233
SiO ₂		-13.1850		-13.1850
Sphalerite	+	.0242	+	.0242

Constituent	Model 7C		Model 7D	
	Input con- straints ³	Out- put	Input con- straints ³	Out- put
Albite	+	0.4950	+	0.4950
Calcite				
Ca-montmorillonite.	+	.1535		
CO ₂ gas		.0015		.0015
Diopside	+	5.6240	+	5.6240
Gibbsite		.3577		
Goethite	-	-7.2405	-	-7.2405
Gypsum	-	-3.7135	-	-3.7376
K-feldspar	+	.1943	+	.1943
MnO ₂	-	-.2380	-	-.2380
NiS	+	.0083	+	.0083
O ₂ gas	+	27.3515	+	27.3996
Pyrite	+	7.2098	+	7.2226
SiO ₂		-13.1850		-13.7484
Sphalerite	+	.0242	+	.0242

¹Blank spaces indicate no figures are relevant.

²Millimoles of reactant or product per kilogram of final water.

³Plus = dissolving; minus = precipitating.

Table A-16.—Input and output files from BALANCE evaluating flow path from well 89-1S to Boyd Seep with mixing of water from well 89-1M, millimoles per kilogram

Element	Final, Boyd Seep	Initial 1, well 89-1S	Initial 2, well 89-1M
Al	2.904	0.0003709	0.003708
C	.001646	5.603	4.301
Ca	11.860	.2939	2.054
Fe	.004317	.0008190	.002188
K	.3057	.08702	.1101
Mg	14.790	.1099	.8207
Mn	1.499	.001359	.0005373
Na	2.836	10.100	.5434
Ni	.05561	.000	.000
RS	218.100	36.340	24.638
S	36.350	2.332	1.239
Si	.5083	.2932	.7260
Zn	.08145	.000	.000

RS Redox state of solution.

Table A-17.—Mineral and gas input data to BALANCE evaluating flow path from well 89-1S to Boyd Seep with mixing of water from well 89-1M

Constituent ¹	Element	Stochastic ratios in empirical formulas
Albite (+)	Na	1.0
	Al	1.0
	Si	3.0
CO ₂ gas (-)	C	1.0
	RS	4.0
Diopside (+)	Ca	1.0
	Mg	1.0
	Si	2.0
Gibbsite (+)	Al	1.0
Goethite (-)	Fe	1.0
	RS	3.0
Gypsum (-)	Ca	1.0
	S	1.0
	RS	6.0
K-feldspar (+) . . .	K	1.0
	Al	1.0
	Si	3.0
MnO ₂ (+)	Mn	1.0
	RS	4.0
NiS (+)	Ni	1.0
	S	1.0
	RS	-2.0
O ₂ gas (+)	RS	4.0
Pyrite (+)	Fe	1.0
	S	1.0
	RS	0.0
SiO ₂	Si	1.0
Sphalerite (+) . . .	Zn	1.0
	S	1.0
	RS	-2.0

RS Redox state of solution.

¹Plus = dissolving; minus = precipitating.

Table A-18.—Mineral and gas output data¹ for model 8A from BALANCE evaluating flow path from well 89-1S to Boyd Seep with mixing of water from well 89-1M

Constituent	Input constraints ²	Output
Initial 1		0.2399
Initial 27601
CO ₂ gas	-	-4.6117
Diopside	+	14.1398
Gibbsite		2.6924
Goethite	-	-19.3092
Gypsum	-	-3.9116
K-feldspar	+	.2087
MnO ₂	+	1.4983
NiS	+	.0556
O ₂ gas	+	71.1949
Pyrite	+	19.3117
SiO ₂		-29.0197
Sphalerite	+	.0814

¹Millimoles of reactant or product per liter of final water, except for initial 1 and initial 2, which are mixing ratios of water that sum to 1.0.

²Plus = dissolving; minus = precipitating.

Table A-19.—Input and output files from BALANCE evaluating mixing of water from well 89-1S with well 89-6-type water to obtain water similar to that found at Boyd Seep, millimoles per kilogram

Element	Final, Boyd Seep	Initial 1, well 89-1S	Initial 2, well 89-6
Al	2.904	0.0003709	0.01112
C001646	5.603	.6671
Ca	11.860	.2939	.1868
Fe004317	.0008190	.0004298
K3057	.08702	.002558
Mg	14.790	.1099	.1088
Mn	1.499	.001359	.0001238
Na	2.836	10.100	.179
RS	218.100	36.340	3.066
S	36.350	2.332	.06621
Si5083	.2932	.3662

RS Redox state of solution.

¹Plus = dissolving; minus = precipitating.

Table A-20.—Mineral and gas input data to BALANCE evaluating mixing of water from well 89-1S with well 89-6-type water to obtain water similar to that found at Boyd Seep

Constituent ¹	Element	Stochastic ratios in empirical formulas
Albite (+)	Na	1.0
	Al	1.0
	Si	3.0
Calcite (+)	Ca	1.0
	C	1.0
	RS	4.0
"CH ₂ O"	C	1.0
CO ₂ gas (-)	C	1.0
	RS	4.0
Diopside (+)	Ca	1.0
	Mg	1.0
	Si	2.0
Gibbsite (+)	Al	1.0
Goethite (-)	Fe	1.0
	RS	3.0
Gypsum (-)	Ca	1.0
	S	1.0
	RS	6.0
Kaolinite (-)	Al	2.0
	Si	2.0
K-feldspar (+)	K	1.0
	Al	1.0
MnO ₂ (+)	Si	3.0
	Mn	1.0
O ₂ gas (+)	RS	4.0
	Fe	1.0
Pyrite (+)	S	2.0
	RS	0.0
	Si	1.0

RS Redox state of solution.

¹Plus = dissolving; minus = precipitating.

Table A-21.—Mineral and gas output data^{1,2} from BALANCE evaluating mixing of water from well 89-1S with well 89-6-type water to obtain water similar to that found at Boyd Seep

Constituent	Model 9A		Model 9B	
	Input con- straints ³	Output	Input con- straints ³	Output
Initial 1		0.0067		0.2678
Initial 29933		.7322
Albite	+	2.5904		
CO ₂ gas	-	-.6986	-	-1.9874
Diopside	+	14.6812	+	14.6809
Gibbsite				2.6152
Goethite	-	-19.6348	-	-19.3529
Gypsum	-	-3.0087	-	-3.0364
K-feldspar	+	.3026	+	.2805
MnO ₂	+	1.4989	+	1.4985
O ₂ gas	+	71.1415	+	71.0888
Pyrite	+	19.6386	+	19.3567
SiO ₂		-37.8987		-30.0417

¹Blank spaces indicate no figures are relevant.

²Millimoles of reactant or product per liter of final water, except for initial 1 and initial 2, which are mixing ratios of water that sum to 1.0.

³Plus = dissolving; minus = precipitating.

Table A-22.—Input and output files from BALANCE evaluating mixing of water from well 89-1S with well 89-6-type water to obtain water similar to that found at Boyd Seep using alternative mineral data, millimoles per kilogram

Element	Final, Boyd Seep	Initial 1, well 89-1S	Initial 2, well 89-6
Al	2.904	0.0003709	0.01112
C001646	5.603	.6671
Ca	11.860	.2939	.1868
Fe004317	.0008190	.0004298
K3057	.08702	.002558
Mg	14.790	.1099	.1088
Mn	1.499	.001359	.0001238
Na	2.836	10.100	.179
RS	218.100	36.340	3.066
S	36.350	2.332	.06621
Si5083	.2932	.3662

RS Redox state of solution.

Table A-23.—Mineral and gas Input data to BALANCE evaluating mixing of water from well 89-1S with well 89-6-type water to obtain water similar to that found at Boyd Seep using alternative mineral data

Constituent ¹	Element	Stochastic ratios in empirical formulas
Albite (+)	Na	1.0
	Al	1.0
	Si	3.0
Anorthite (+)	Ca	1.0
	Al	2.0
CO ₂ gas (-)	Si	2.0
	C	1.0
Dolomite (+)	RS	4.0
	Ca	1.0
	Mg	1.0
	C	1.0
	RS	8.0
	Al	1.0
Gibbsite (+)	Al	1.0
Goethite (-)	Fe	1.0
	RS	3.0
Gypsum (-)	Ca	1.0
	S	1.0
	RS	6.0
	Al	2.0
Kaolinite (-)	Si	2.0
	K	1.0
K-feldspar (+)	Al	1.0
	Si	3.0
MnO ₂ (+)	Mn	1.0
	RS	4.0
O ₂ gas (+)	RS	4.0
	Fe	1.0
Pyrite (+)	S	2.0
	RS	0.0
SiO ₂	Si	1.0

RS Redox state of solution.

¹Plus = dissolving; minus = precipitating.

Table A-24.—Mineral and gas output data¹ for model 10A from BALANCE evaluating mixing of water from well 89-1S with well 89-6-type water to obtain water similar to that found at Boyd Seep using alternative mineral data

Constituent	Input constraints ²	Output
Initial 1		0.2678
Initial 27322
Anorthite	+	1.3076
CO ₂ gas		-31.3492
Dolomite	+	14.6809
Goethite	-	-20.0067
Gypsum	-	-4.3440
K-feldspar	+	.2805
MnO ₂	+	1.4985
O ₂ gas	+	73.5405
Pyrite	+	20.0105
SiO ₂		-3.2952

¹Millimoles of reactant or product per kilogram of final water, except for initial 1 and initial 2, which are mixing ratios of water that sum to 1.0.

²Plus = dissolving; minus = precipitating.

Table A-25.—Saturation Indices for selected minerals from WATEQ4F using analytical data from Sis Pool

Mineral	
Albite	-9.199
Allophane	-.578
Anorthite	-21.291
Ca-montmorillonite	-7.321
Diopside	-20.725
Ferrihydrite	-5.246
Gibbsite	-4.003
Goethite647
Gypsum058
Jarosite K	-9.026
Jurbanite	1.095
Kaolinite	-4.285
K-mica	-10.156
Manganite	-11.686
Melanterite	-2.704
Pyrolusite	-18.999
Silica (amorphous)114

Table A-26.—Input and output files from BALANCE evaluating quantity of minerals consumed in protore pile to produce water at Sis Pool from infiltration water (well 89-6-type water), millimoles per kilogram

Element	Final, Sis Pool	Initial, well 89-6
Al	59.100	0.01112
C000	.6671
Ca	10.390	.1868
Fe	2.580	.0004298
K03921	.002558
Mg	53.090	.1088
Mn	11.190	.0001238
Na6243	.1790
RS	1,109.0	3.066
S	184.800	.06621
Si	1.772	.3662
Zn5289	.000

RS Redox state of solution.

Table A-27.—Mineral and gas Input data to BALANCE evaluating quantity of minerals consumed in protore pile to produce water at Sis Pool from infiltration water (well 89-6-type water)

Constituent ¹	Element	Stochastic ratios in empirical formulas
Albite (+)	Na	1.0
	Al	1.0
	Si	3.0
Calcite (+)	Ca	1.0
	C	1.0
	RS	4.0
CO ₂ gas (-)	C	1.0
	RS	4.0
Diopside (+)	Ca	1.0
	Mg	1.0
	Si	2.0
	Al	1.0
	RS	3.0
Gypsum (-)	Ca	1.0
	S	1.0
	RS	6.0
K-feldspar (+)	K	1.0
	Al	3.0
	Si	3.0
	Mn	1.0
MnO ₂ (+)	RS	4.0
	RS	4.0
O ₂ gas (+)	RS	4.0
	Fe	1.0
Pyrite (+)	S	2.0
	RS	0.0
	Si	1.0
Sphalerite (+)	Zn	1.0
	S	1.0
	RS	-2.0

RS Redox state of solution.

¹Plus = dissolving; minus = precipitating.

Table A-28.—Mineral and gas output data¹ for model 12A from BALANCE evaluating quantity of minerals consumed in protore pile to produce water at Sis Pool from infiltration water (well 89-6-type water)

Constituent	Input constraints ²	Output
Albite	+	0.4453
CO ₂ gas	-	-.6671
Diopside	+	52.9812
Gibbsite	+	58.6069
Goethite	-	-110.9119
Gypsum	-	-42.7780
K-feldspar	+	.0367
MnO ₂	+	11.1899
O ₂ gas	+	413.5761
Pyrite	+	113.4914
SiO ₂		-106.0025
Sphalerite	+	.5289

¹Millimoles of reactant or product per kilogram of final water.

²Plus = dissolving; minus = precipitating.

Table A-29.—Input and output files from BALANCE comparing mixing ratios of infiltration water and pumpback water from pollution control pond to produce water found in pit 3, millimoles per kilogram

Element	Final, pit 3	Initial 1, pollution control pond	Initial 2, well 89-6
Al	1.857	3.728	0.01112
C	.000164	.001647	.6671
Ca	9.948	11.65	.1868
Fe	.02228	.0188	.0004298
K	.1114	.1799	.002558
Mg	9.166	16.99	.1088
Na	2.341	1.735	.1790
RS	153.67	231.18	3.066
S	25.61	38.53	.06621
Si	.3774	.6824	.3662

RS Redox state of solution.

Table A-30.—Mineral and gas Input data to BALANCE comparing mixing ratios of infiltration water and pumpback water from pollution control pond to produce water found in pit 3

Constituent ¹	Element	Stochastic ratios in empirical formulas
Albite (+)	Na	1.0
	Al	1.0
	Si	3.0
Calcite (+)	Ca	1.0
	Mg	1.0
	RS	4.0
CO ₂ gas (-)	C	1.0
	RS	4.0
Diopside (+)	Ca	1.0
	Mg	1.0
	Si	2.0
Gibbsite (+)	Al	1.0
Goethite (-)	Fe	1.0
	RS	3.0
Gypsum	Ca	1.0
K-feldspar (+)	K	1.0
	Al	1.0
	Si	3.0
O ₂ gas	RS	4.0
Pyrite (+)	Fe	1.0
	S	2.0
	RS	0.0
SiO ₂	Si	1.0

RS Redox state of solution.
¹Plus = dissolving; minus = precipitating.

Table A-31.—Mineral and gas output data¹ for model 13A from BALANCE comparing mixing ratios of infiltration water and pumpback water from pollution control pond to produce water found in pit 3

Constituent	Input constraints ²	Output
Initial 1		0.5365
Initial 2		.4635
Albite	+	1.3272
Calcite	+	3.6109
CO ₂ gas	-	-3.9208
Gibbsite		-1.4892
Goethite	-	-2.4415
K-feldspar	+	.0137
O ₂ gas		9.1948
Pyrite	+	2.4535
SiO ₂		-4.1810

¹Millimoles of product or reactant per kilogram of final water, except for initial 1 and initial 2, which are mixing ratios of water that sum to 1.00.

²Plus = dissolving; minus = precipitating.

Table A-32.—Saturation Indices for selected minerals from WATEQ4F using analytical data from pit 4 and pit 3 seep

Mineral	Pit 4	Pit 3 seep
Albite	-1.375	-0.817
Allophane	-.549	-.035
Anorthite	-2.721	-2.326
Calcite	.218	-.164
Ca-montmorillonite	1.955	3.849
Diopside	-1.114	-3.067
Dolomite	-.579	-1.105
Ferrihydrite	1.994	2.259
Gibbsite	.449	1.113
Goethite	7.885	8.150
Gypsum	-.920	-.567
Jarosite K	-5.064	-1.729
Kaolinite	3.005	4.633
K-mica	6.859	8.616
Manganite	2.354	.583
Silica (amorphous)	-.679	-.529

Table A-33.—Input and output files from BALANCE evaluating possible flow path from pit 4 to pit 3 seep with mixing of well 89-6 water, millimoles per kilogram

Element	Final, pit 3 seep	Initial 1, pit 4	Initial 2, well 89-6
Al	0.010	0.000	0.000
C	1.401	.9003	.6671
Ca	5.015	2.916	.1868
Fe	.001156	.0004838	.0004298
K	.0969	.08957	.002558
Mg	3.473	1.185	.1088
Mn	.3170	.007286	.0001238
Na	1.080	.7530	.1790
RS	55.632	28.285	3.066
S	8.338	4.114	.06621
Si	.4306	.3081	.3662

RS Redox state of solution.

Table A-34.—Mineral and gas input data to BALANCE evaluating possible flow path from pit 4 to pit 3 seep with mixing of well 89-6 water

Constituent ¹	Element	Stochastic ratios in empirical formulas
Albite (+)	Na	1.0
	Al	1.0
	Si	3.0
Calcite (+)	Ca	1.0
	C	1.0
	RS	4.0
	C	1.0
CO ₂ gas	RS	4.0
	Ca	1.0
Diopside (+)	Mg	1.0
	Si	2.0
	Al	1.0
	Fe	1.0
Gibbsite (-)	RS	3.0
	Ca	1.0
Goethite (-)	S	1.0
	RS	6.0
	Al	2.0
Kaolinite (-)	Si	2.0
	K	1.0
	Al	1.0
K-feldspar (+)	Si	3.0
	Mn	1.0
	RS	4.0
MnO ₂ (+)	RS	4.0
	RS	4.0
O ₂ gas (+)	Fe	1.0
	S	2.0
Pyrite (+)	RS	0.0
	Si	1.0

RS Redox state of solution.

¹Plus = dissolving; minus = precipitating.

Table A-35.—Mineral and gas output data^{1,2} from BALANCE evaluating possible flow path from pit 4 to pit 3 seep with mixing of well 89-6 water

Constituent	Model 15A		Model 15B	
	Input con-straints ³	Out-put	Input con-straints ³	Out-put
Initial 1		0.5142		0.8857
Initial 2		.4858		.1143
Albite	+	.6058	+	.3926
Calcite	+	.6140		
CO ₂ gas				.5274
Diopside	+	2.8108	+	2.4111
Dolomite				
Gibbsite				
Goethite			-	-2.3427
Kaolinite	-	-.3251	-	-.2005
K-feldspar	+	.0496	+	.0173
MnO ₂	+	.3132	+	.3105
O ₂ gas	+	11.2931	+	8.4768
Pyrite	+	3.0952	+	2.3434
SiO ₂		-6.8433		-5.5349

Model 15C		
Input con-straints ³	Out-put	
Initial 1	0.8857	
Initial 2	.1143	
Albite	+	.3926
Calcite		
CO ₂ gas		-4.2947
Diopside		
Dolomite	+	2.4111
Gibbsite	-	-.4011
Goethite	-	-2.3423
Kaolinite		
K-feldspar	+	.0173
MnO ₂	+	.3105
O ₂ gas	+	8.4769
Pyrite	+	2.3430
SiO ₂		-1.1139

¹Blank spaces indicate no figures are relevant.

²Millimoles of product or reactant per kilogram of final water, except for initial 1 and initial 2, which are mixing ratios of water that sum to 1.00.

³Plus = dissolving; minus = precipitating.

Table A-36.—Saturation indices for selected minerals from WATEQ4F using analytical data from well 89-3M and well 89-3D

Mineral	Well 89-3M	Well 89-3D
Albite	-0.331	-0.913
Allophane	.615	.851
Anorthite	-2.968	-1.374
Calcite	-1.808	-.850
Ca-montmorillonite	7.652	6.245
Diopside	-10.022	-7.207
Ferrihydrite	2.795	1.467
Gibbsite	2.595	2.723
Goethite	8.688	7.359
Gypsum	.062	-1.013
Jarosite K	7.631	-2.417
Kaolinite	8.162	7.265
K-mica	11.970	11.647
Manganite	-4.571	-.880
Pyrolusite	-9.927	-3.838
Silica (amorphous)	-.246	-.821
ZnSiO ₃	-.085	.371

Table A-37.—Saturation indices for selected minerals from WATEQ4F using analytical data from well 89-4S and South Spoils Seep

Mineral	Well 89-4S	South Spoils Seep
Albite	-6.345	-7.450
Allophane	-.988	-.901
Al (OH) ₃	-3.764	-5.329
Anorthite	-13.688	-17.528
Calcite	-6.631	
Ca-montmorillonite	-2.170	-4.580
Diopside	-16.906	-18.802
Ferrihydrite	-7.704	-5.720
Gibbsite (crystalline)	-.938	-2.495
Goethite	-1.812	.172
Gypsum	.038	.073
Jarosite K	-20.192	-12.306
Jurbanite	1.306	1.275
Kaolinite	.507	-1.805
K-mica	-.978	-5.388
Manganite	-13.824	-10.438
Pyrolusite	-25.768	-18.030
Quartz	.810	1.213
Silica (amorphous)	-.555	-.159

Table A-38.—Input and output files from BALANCE evaluating possible flow path from well 89-4S to South Spoils Seep with mixing of well 89-6-type water, millimoles per kilogram

Element	Final, South Spoils Seep	Initial 1, well 89-4S	Initial 2, well 89-6-type
Al	17.390	3.598	0.01112
C	.000	.001649	.6671
Ca	11.080	11.520	.1868
Fe	.04344	.5403	.0004298
K	.09401	.1615	.002558
Mg	34.440	19.020	.1088
Mn	9.260	4.835	.0001238
Na	1.558	1.714	.1790
RS	561.8	281.5	3.066
S	93.63	46.910	.06621
Si	.9494	.3968	.3662
Zn	.3530	.1087	.000

RS Redox state of solution.

Table A-39.—Mineral and gas input data to BALANCE evaluating possible flow path from well 89-4S to South Spoils Seep with mixing of well 89-6-type water

Constituent ¹	Element	Stochastic ratios in empirical formulas
Albite (+)	Na	1.0
	Al	1.0
	Si	3.0
Calcite (+)	Ca	1.0
	C	1.0
	RS	4.0
CO ₂ gas	C	1.0
	RS	4.0
Diopside (+)	Ca	1.0
	Mg	1.0
	Si	2.0
Gibbsite	Al	1.0
Goethite (-)	Fe	1.0
	RS	3.0
Gypsum (-)	Ca	1.0
	S	1.0
	RS	6.0
Kaolinite (+)	Al	2.0
	Si	2.0
K-feldspar (+)	K	1.0
	Al	1.0
	Si	3.0
MnO ₂ (+)	Mn	1.0
	RS	4.0
O ₂ gas	RS	4.0
Pyrite (+)	Fe	1.0
	S	2.0
	RS	0.0
SiO ₂	Si	1.0
Sphalerite (+)	Zn	1.0
	S	1.0
	RS	-2.0

RS Redox state of solution.

¹Plus = dissolving; minus = precipitating.

Table A-40.—Mineral and gas output data¹ for model 18A from BALANCE evaluating possible flow path from well 89-4S to South Spoils Seep with mixing of well 89-6-type water

Constituent	Input constraints ²	Output
Initial 1		0.5754
Initial 2		.4246
Albite	+	.4958
CO ₂ gas		-.2842
Diopside	+	23.4501
Goethite	-	-42.9669
Gypsum	-	-19.0778
Kaolinite	+	7.4096
MnO ₂	+	6.4780
O ₂ gas	+	154.4260
Pyrite	+	42.6993
SiO ₂		-62.6412
Sphalerite	+	.2900

¹Millimoles of product or reactant per kilogram of final water, except for initial 1 and initial 2, which are mixing ratios of water that sum to 1.00.

²Plus = dissolving; minus = precipitating.

Table A-41.—Saturation indices for selected minerals from WATEQ4F using analytical data from East Drainage Control and East Drainage 11

Mineral	East Drainage Control	East Drainage 11
Albite	-0.347	0.002
Allophane	.201	.038
Anorthite	-1.874	-1.620
Calcite	.374	.855
Ca-montmorillonite	4.829	4.432
Diopside	-2.646	-.923
Ferrihydrite	2.181	2.561
Gibbsite	1.074	.800
Goethite	8.072	8.452
Gypsum	-1.928	-.900
Jarosite K	-5.700	-3.581
Kaolinite	5.147	4.665
K-mica	9.328	9.197
Manganite	1.500	1.396
Pyrolusite	-.915	-.645
Silica (amorphous)	.097	.129

Table A-42.—Input and output files from BALANCE evaluating flow path from East Drainage Control to East Drainage 11 with mixing of water from Boyd Seep, millimoles per minute¹

Element	Final, East Drainage 11	Initial 1, East Drainage Control	Initial 2, Boyd Seep
Al	0.020	0.010	6.093
C	88.040	43.010	.0009053
Ca	79.440	18.960	6.523
Fe	.0186	.004658	.02374
Mg	30.580	5.569	8.134
Mn	.05822	.3387	.8245
Na	10.046	2.757	1.5598
RS	751.600	196.600	119.960
S	66.560	4.086	19.990
Si	17.120	8.092	.2796

RS Redox state of solution.

¹To convert from millimoles per kilogram to millimoles per minute, a flow rate of 76 L/min was used for East Drainage 11, 38 L/min for East Drainage Control, and 2 L/min for Boyd Seep.

Table A-43.—Mineral and gas Input data to BALANCE evaluating flow path from East Drainage Control to East Drainage 11 with mixing of water from Boyd Seep

Constituent ¹	Element	Stochastic ratios in empirical formulas
Albite (+)	Na	1.0
	Al	1.0
	Si	3.0
Anorthite (+)	Ca	1.0
	Al	2.0
	Si	2.0
Calcite (+)	Ca	1.0
	C	1.0
	RS	4.0
CO ₂ gas	C	1.0
	RS	4.0
Diopside (+)	Ca	1.0
	Mg	1.0
	Si	2.0
Dolomite (+)	Ca	1.0
	Mg	1.0
	C	2.0
	RS	8.0
Gibbsite	Al	1.0
Goethite (-)	Fe	1.0
	RS	3.0
MnOOH (+)	Mn	1.0
	RS	2.0
O ₂ gas	RS	4.0
Pyrite (+)	Fe	1.0
	S	2.0
	RS	0.0
SiO ₂	Si	1.0

RS Redox state of solution.

¹Plus = dissolving; minus = precipitating.

Table A-44.—Mineral and gas output data¹ for model 20A from BALANCE evaluating flow path from East Drainage Control to East Drainage 11 with mixing of water from Boyd Seep

Constituent	Input constraints ²	Output
Initial 1	+	0.8963
Initial 2	+	.1037
Albite	+	7.4131
Anorthite	+	37.0247
Dolomite	+	24.7450
Gibbsite		-82.0834
Goethite	-	30.4006
MnOOH	-	-.3309
O ₂ Gas	+	114.2127
Pyrite	+	30.4124
SiO ₂		-86.4507

¹Millimoles of product or reactant per minute, except for initial 1 and initial 2, which are mixing ratios of water that sum to 1.00. To convert from millimoles per kilogram to millimoles per minute, a flow rate of 76 L/min was used for East Drainage 11, 38 L/min for East Drainage Control, and 2 L/min for Boyd Seep.

²Plus = dissolving; minus = precipitating.

Table A-45.—Saturation indices for selected minerals from WATEQ4F using analytical data from West Drainage Control and well 89-7

Mineral	West Drain- age Control	Well 89-7
Albite	-4.654	-0.570
Allophane	-.740	.472
Anorthite	-10.848	-1.699
Calcite	-7.061	-1.521
Ca-montmorillonite193	7.031
Diopside	-14.636	-8.167
Ferrihydrite	-4.188	1.071
Gibbsite	-.295	2.465
Goethite	1.704	6.962
Gypsum	-.013	-1.210
Jarosite K	-10.605	-1.720
Kaolinite	2.155	7.559
K-mica	2.055	11.582
Manganite	-8.617	-5.264
Pyrolusite	-14.853	-8.663
Silica (amorphous)	-.022	-.068